The Zonally Averaged Transport Characteristics of the GFDL General Circulation/Transport Model

R. A. PLUMB

Geophysical Fluid Dynamics Program, Princeton University, Princeton, NJ 08542
and
CSIRO Division of Atmospheric Research, Aspendale, 3195, Australia

J. D. MAHLMAN

Geophysical Fluid Dynamics Laboratory/NOAA, Princeton University, Princeton NJ 08542

ABSTRACT

The GFDL general circulation/tracer model has been used to generate the transport coefficients required in two-dimensional (zonally averaged) transport formulations. This was done by assuming a flux-gradient relationship and then, given gradient and flux statistics from two independent (and contrived) model tracer experiments, to derive the coefficients by inversion of this relation. Given the mean meridional circulation from the GCM, the antisymmetric and symmetric parts of the coefficients tensor determine the advective and diffusive contributions to the net meridional transport in the model. The effective transport circulation thus defined differs substantially from the Lagrangian mean and residual circulations and is in fact a simpler representation of the model circulation than either of these. The diffusive component is coherently structured, comprising the following components:

(i) Strong quasi-horizontal mixing ($D_{yy} \sim 1 \times 10^6$ m^2 s^{-1}) in the midlatitude lower troposphere, apparently associated with fronts and the occlusion of synoptic systems.

(ii) A band of strong quasi-horizontal mixing ($D_{yy} \sim 2 \times 10^6$ m^2 s^{-1}) stretching across the tropical upper troposphere and the subtropical winter stratosphere. This band follows the band of weak zonal mean winds and is a manifestation in the model of the "surf zone" recently identified by McIntyre and Palmer as a region of breaking planetary waves. Outside the "surf zone," $D_{yy} \lesssim 5 \times 10^5$ m^2 s^{-1} in the stratosphere, consistent with other recent estimates.

(iii) Intense vertical mixing ($D_{zz} \gtrsim 10$ m^2 s^{-1}) in the troposphere at and near the latitudes of the intertropical convergence zone.

(iv) Vertical mixing ($D_{zz} \sim 5$–10 m^2 s^{-1}) through much of the troposphere, a substantial component of which is associated with subgrid-scale mixing (model convective processes).

The validity of the flux-gradient relation as a parameterization of eddy transport processes was tested by implementing the parameterization in a two-dimensional model, using these derived coefficients. In comparison experiments it was found that the two-dimensional model could reproduce well the zonally-averaged evolution of tracers in the GCM; the quantitative errors that were found may in part result from the finite model resolution, rather than from errors in formulation. Therefore, although the flux-gradient relation is formally justified only in the small-amplitude limit, it appears to be a useful practical description of large-scale transport by finite-amplitude eddies.

1. Introduction

Chemical/dynamical models of global constituent budgets range in complexity from three-dimensional general circulation models through reducing dimensions to two, one and even zero dimensional models. While the three-dimensional transport model undoubtedly provides the most sophisticated and most precise approach it is still relatively expensive—especially if the chemistry is complex—and demanding in terms of computer facilities and modeling expertise. Therefore many workers continue to focus their modeling efforts on reduced-dimension models in which some aspects of atmospheric transport are parameterized rather than explicitly represented. Of these models, the two-dimensional, zonally-averaged, model has become widespread.

There are several reasons for the popularity of the zonally-averaged approach. The first of these is, of course, the greatly reduced size and complexity of such models (as compared with a three dimensional model). Second, for many purposes, the modeling of the zonal structure of atmospheric constituents is of secondary importance. Since, in most of the atmosphere, winds are predominantly zonal, transport in the zonal direction (albeit along wavy trajectories) is relatively rapid so that most structure is in the meridional plane. A third reason is increasing confidence in the parame-

terization of eddy transport processes. This has traditionally been effected via a flux-gradient relation. While earlier formulation and application of this relation is now recognized as being invalid, more recent developments have formally justified a flux-gradient relationship for small-amplitude eddies. Nevertheless, the transport coefficients which appear in this relation are functions of Lagrangian eddy statistics which are not easy to determine from atmospheric circulation data. Some attempts to construct zonally-averaged models have therefore relied on simplifying assumptions which circumvent this requirement or which permit the estimation of the coefficients from Eulerian data. However it will be argued in this paper (section 3) that some of these assumptions are theoretically ill-founded and that there is, a priori, little reduction that can be effected in the complexity of the problem.

The approach adopted here, and described in sections 4 and 5, is to assume the validity of the flux-gradient relation and thence to deduce the transport coefficients by inversion of that relation, thus circumventing the need to obtain Lagrangian statistics. Even so, the data requirements cannot be met by available atmospheric data. However, it is straightforward to obtain data in the required form from general circulation models; the GFDL general circulation/tracer model was used for this purpose. Of course, this model like any other has its limitations as a surrogate atmosphere; however, it should be emphasized that the major objectives of this study are not seriously undermined by errors in the model transport. Basically, this study establishes a two-dimensional description of the three-dimensional model in order to:

(i) provide insight into the dynamical processes which determine zonally-averaged transport in the model,

(ii) Allow—to the authors' knowledge for the first time—an objective basis for assessing the practical validity of the flux-gradient parameterization, and

(iii) generate a set of transport coefficients which may be useful as input to two-dimensional transport models.

Of these objectives, the first two are largely independent of inadequacies in the GCM transport (provided the GCM representation of the atmosphere is at all reasonable). The relevance of these results to atmospheric transport calculations is of course limited by the deficiencies of the GCM; the advantage of a GCM approach is the objectivity it permits which, at the present state of the art, may make the approach at least competitive with less objective procedures to estimate transport coefficients from real data.

Finally, the derived coefficients were tested by using them in a two-dimensional model and comparing the predictions of this model with the zonally-averaged fields produced in parallel experiments with the parent general circulation model. As discussed in section 6,

agreement is generally good. This result serves to validate not only these calculations but also the relevance of the flux-gradient relation, despite the fact that the assumptions on which the flux-gradient parameterization is based (i.e. that the eddies are of small amplitude) are far from satisfied.

2. The flux-gradient relation and definition of the transport coefficients

Consider a quasi-conserved constituent whose mixing ratio q satisfies the equation

$$\frac{dq}{dt} = s \qquad (2.1)$$

where s represents sources and/or sinks. These may be chemical or photochemical creation or destruction processes, or molecular diffusion. Indeed, if the former processes are weak, then diffusion must become a substantial term in (2.1) since distortion and stretching of material lines by the motion must then inevitably cause a cascade of q variance down to small scales, just as for a dynamical quantity like potential vorticity (e.g., see Danielsen, 1981; Holloway and Kristmannsson, 1984; McIntyre and Palmer, 1984; Mahlman, 1985).

The zonally-averaged budget equation may be written, in sine-latitude coordinates,

$$\frac{\partial \bar{q}}{\partial t} + \bar{v}\cos\phi\frac{\partial \bar{q}}{\partial y} + \bar{w}\frac{\partial \bar{q}}{\partial z} = \bar{s} - \frac{1}{p}\nabla\cdot\mathbf{F} \qquad (2.2)$$

where p is pressure, ϕ is latitude, $y = a\sin\phi$ (where a is the Earth's radius), z is the log-pressure coordinate $H\ln[(1000\ mb)/p]$ where H is a constant scale-height and

$$\mathbf{F} = (F_y, F_z) = (\overline{pv'q'}, \overline{pw'q'}) \qquad (2.3)$$

is the eddy flux (where the prime denotes the departure from a zonal average). In these coordinates the flux divergence is $\nabla\cdot\mathbf{F} = \partial(F_y\cos\phi)/\partial y + \partial F_z/\partial z$ and the zonal mean circulation may, by virtue of the continuity equation $\partial(p\bar{v}\cos\phi)/\partial y + \partial(p\bar{w})/\partial z = 0$ be written in terms of a streamfunction χ, viz:

$$p\bar{v}\cos\phi = -\frac{\partial(p\chi)}{\partial z}; \quad \bar{w} = \frac{\partial\chi}{\partial y}. \qquad (2.4)$$

In order to obtain a zonally-averaged closure of (2.2), the eddy flux must be parameterized in terms of zonally-averaged quantities. This usually proceeds by means of a flux-gradient relation which we write here in the form

$$(F_y\cos\phi, F_z) = -p\mathbf{K}\cdot\nabla\bar{q} \qquad (2.5)$$

where

$$\mathbf{K} = \begin{bmatrix} K_{yy} & K_{yz} \\ K_{zy} & K_{zz} \end{bmatrix} \qquad (2.6)$$

This type of relation has long been in use (e.g., Lettau, 1951) but it is only relatively recently that it has been

justified for small-amplitude, but otherwise general, eddy motions on a zonal flow (Plumb, 1979, Matsuno, 1980). Thus it has been shown that the transport tensor $\mathbf{K}$ may conveniently be regarded as comprised of two parts

$$\mathbf{K} = \mathbf{L} + \mathbf{D} \tag{2.7}$$

where $\mathbf{L}$ and $\mathbf{D}$ are respectively antisymmetric and symmetric tensors whose components may be expressed in terms of the parcel displacement (ξ, η, ζ) defined in the generalized Lagrangian-mean theory of Andrews and McIntyre (1978). Specifically

$$\mathbf{L} = \begin{bmatrix} 0 & \frac{1}{2}(\overline{v'\zeta} - \overline{w'\eta}) \\ \frac{1}{2}(\overline{w'\eta} - \overline{v'\zeta}) & 0 \end{bmatrix} \tag{2.8}$$

and, for a conserved tracer ($s = 0$),

$$\mathbf{D} = \begin{bmatrix} \dfrac{\partial}{\partial t}(\frac{1}{2}\overline{\eta^2}) & \dfrac{\partial}{\partial t}(\frac{1}{2}\overline{\eta\zeta}) \\ \dfrac{\partial}{\partial t}(\frac{1}{2}\overline{\eta\zeta}) & \dfrac{\partial}{\partial t}(\frac{1}{2}\overline{\zeta^2}) \end{bmatrix} \tag{2.9}$$

If q is not exactly conserved, (and it was noted above that it never will be) then other terms must be added to (2.9); for example if s is a weak relaxation such that $s' = -\lambda q'$ and if the parcel displacement statistics are steady, then (2.9) contains an additional term

$$\mathbf{D} = \begin{bmatrix} \lambda\overline{\eta^2} & \lambda\overline{\eta\zeta} \\ \lambda\overline{\eta\zeta} & \lambda\overline{\zeta^2} \end{bmatrix} \tag{2.10}$$

(Plumb, 1979; Matsuno, 1980; Pyle and Rogers, 1980a; Danielsen, 1981). Because of its symmetry, $\mathbf{D}$ can be made purely diagonal via a local coordinate rotation to its principal axes. If we rotate coordinates through an angle α where

$$\tan 2\alpha = \frac{2D_{yz}}{D_{yy} - D_{zz}} \tag{2.11}$$

then, in the new coordinates,

$$\mathbf{D}' = \begin{bmatrix} D'_{yy} & 0 \\ 0 & D'_{zz} \end{bmatrix} \tag{2.12}$$

where

$$\left. \begin{aligned} D'_{yy} &= \cos^2\alpha D_{yy} + \sin^2\alpha D_{zz} + 2\sin\alpha\,\cos\alpha D_{yz} \\ D'_{zz} &= \sin^2\alpha D_{yy} + \cos^2\alpha D_{zz} - 2\sin\alpha\,\cos\alpha D_{yz} \end{aligned} \right\}. \tag{2.13}$$

Provided $D_{yy} \geq 0$, $D_{zz} \geq 0$ and $D_{yz}^2 \leq D_{yy}D_{zz}$, then $D'_{yy} \geq 0$ and $D'_{zz} \geq 0$ and the component of the eddy flux associated with $\mathbf{D}$ is purely diffusive (Matsuno, 1980).

The purely kinematic terms in (2.9) reflect the diffusive transport via simple dispersion of air parcels. While these dispersion terms are time-derivatives of parcel displacement statistics they do not (contrary to assumptions underlying some approaches to stratospheric transport modeling) necessarily vanish when the Eulerian flow statistics are steady. This fact had

long been recognised in classical turbulence theory (e.g., in parameterizations of the atmospheric boundary layer) and, indeed, the sustained dispersion of air parcels in statistically steady flow is the very essence of turbulent transport.

The structure of the nonconservative contribution (2.10), is similar to that of (2.9), but with the relaxation rate replacing the dispersion rate. Since the former differs for different constituents, so in principle do the diffusion coefficients. This apparently undermines any attempt to derive a universal parameterization of eddy transport although some progress can be made for simple motions (e.g., Hartmann and Garcia, 1979; Tung, 1984). In fact, the situation becomes even more complex if two or more constituents interact, although this can to some extent be circumvented by restricting attention to families of constituents (Pyle and Rogers, 1980a). Any hope of recovering a universal transport parameterization hinges on the diffusion being dominated by kinematic dispersion.

The contribution to the eddy flux associated with the antisymmetric tensor $\mathbf{L}$ is quite different in character; this flux is directed normal to the $\bar{q}$ gradient (Clark and Rogers, 1978) and is advective, rather than diffusive (Plumb, 1979; Matsuno, 1980; Danielsen, 1981). Using (2.7) in (2.5), (2.2) may be written

$$\frac{\partial \bar{q}}{\partial t} + V_T\cos\phi\frac{\partial \bar{q}}{\partial y} + W_T\frac{\partial \bar{q}}{\partial z} = \bar{s} + \frac{1}{p}\nabla\cdot(p\mathbf{D}\cdot\nabla\bar{q}) \tag{2.14}$$

where $\mathbf{U}_T = (V_T, W_T)$ is an effective transport velocity which is defined by

$$V_T\cos\phi = -\frac{1}{p}\frac{\partial}{\partial z}(p\chi_T); \quad W_T = \frac{\partial\chi_T}{\partial y} \tag{2.15}$$

where the streamfunction is

$$\chi_T = \chi - \frac{1}{2}(\overline{v'\zeta} - \overline{w'\eta}). \tag{2.16}$$

Note that this circulation is not in general the same as the Lagrangian-mean velocity $\bar{u}^L$ of Andrews and McIntyre (1978). The physical significance of $\mathbf{U}_T$ and the reasons for the difference between $\mathbf{U}_T$ and $\bar{u}^L$ when $\mathbf{D}$ is spatially inhomogeneous may be understood from Fig. 1. Consider at some initial instant a localized distribution of $\bar{q}$ at point A. Some short time δt later the distribution of $\bar{q}$ occupies the stippled region; in the context of (2.14) we may define a reference point B, which moves with the velocity $\mathbf{U}_T$ and about which $\bar{q}$ diffuses. Thus the location of B relative to A is $\mathbf{U}_T\delta t$. However if the diffusion about B is nonuniform, the distribution of $\bar{q}$ becomes skewed. In Fig. 1 it has been assumed for simplicity that the diffusion is independent of z but that D_{yy} increases locally with y and hence the center of mass of the tracer distribution is located at C, to the right of B. Since $\bar{u}^L$ is the velocity of the center of mass of the distribution (Andrews and McIntyre 1978) the location of C relative to A is $\bar{u}^L\delta t$, and there-
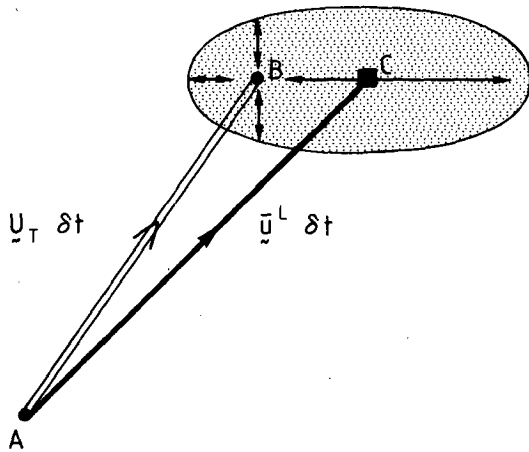
FIG. 1. Illustrating the difference between the transport circulation U_T and Lagrangian mean circulation $\bar{u}^L$ in the presence of inhomogeneous diffusion. The reference point B moves with the transport circulation; the center of mass C moves with the Lagrangian mean velocity. If the diffusion about B is inhomogeneous, C moves relative to B and therefore the two velocities differ under such circumstances. See text for discussion.

fore $\bar{u}^L \neq U_T$. The two are equal only when the diffusion is spatially homogeneous. In fact, $\bar{u}^L$ is otherwise not a nondivergent velocity [see (5.3) and discussion thereof below], whereas U_T always satisfies the continuity equation $\nabla \cdot (p U_T) = 0$, by the definition (2.15). The transport circulation defined by U_T appears to be the same as the "advective mass flux" identified by Kida (1983a) as the time-reversible component of the transport.

In general, χ_T differs also from the stream function χ_* of the residual circulation, defined by (Andrews and McIntyre, 1976)

$$\chi_* = \chi + \frac{\overline{v'\theta'}}{\partial \bar{\theta}/\partial z},\qquad (2.17)$$

where θ is potential temperature. Since θ is a quasi-conserved quantity, we may use (2.5), with (2.3), (2.7) and (2.8) to deduce that

$$\overline{v'\theta'} = -D_{yy}\frac{\partial\bar{\theta}}{\partial y} - \left[D_{yz} + \frac{1}{2}(\overline{v'\zeta} - \overline{w'\eta})\right]\frac{\partial\bar{\theta}}{\partial z}$$

and then, using (2.16) and (2.17), that

$$\chi_* = \chi_T - D_{yy}\frac{\partial\bar{\theta}/\partial y}{\partial\bar{\theta}/\partial z} - D_{yz}\qquad (2.18)$$

The conditions under which $\chi_T \approx \chi_*$ and an interpretation of the difference between the two circulations in general will be discussed below.

3. Determination of the transport coefficients

While the transport coefficients may thus be defined in terms of Lagrangian parcel statistics, their determination on this basis is a difficult problem. Such statistics are not, of course, available directly from the routine observational network, nor is it likely to be a profitable approach to try to infer them from Eulerian statistics of, for example, velocity variances. (Some further difficulties associated with the practical application of generalized Lagrangian-mean theory are discussed by McIntyre, 1980, and Dunkerton, 1980). This direct approach becomes possible, though still difficult, in numerical models where one can generate the required statistics; some gross estimates of D_{yy} for the stratosphere of a hemispheric model have thus been made by Kida (1983a).

Most previous attempts to estimate the coefficients have relied on some simplifying assumptions to reduce the complexity of the problem. Thus Reed and German (1965), in their pioneering study, assumed the parcel orbits to be linearly polarized; this implies a purely diffusive transport tensor with the diffusion being locally along the direction of the parcel displacements. However, it is now recognized that such orbits are atypical of large-scale atmospheric eddies (Wallace, 1978; Matsuno, 1980) and the "diffusion only" parameterization is now little used.

More recently, some approaches (e.g., Holton, 1981; Garcia and Solomon, 1983; Guthrie et al., 1984; Solomon and Garcia, 1984; Tung, 1984; Ko et al., 1985) have tended toward the opposite extreme, in which net transport of stratospheric constituents is regarded as being dominated by the advective transport of the residual or diabatic circulation. Thus, the diffusive component of the eddy transport is relegated almost to the role of subgrid diffusion in general circulation models, which dissipates the small-scale variance generated by the large-scale deformation fields without having any appreciable direct impact on the larger scales. This approach, however, seems incompatible with the transformed Eulerian-mean momentum budget in midlatitudes which for inviscid, steady, quasi-geostrophic flow may be written (e.g., Edmon et al. 1980).

$$f\bar{v}_* = \overline{v'Q'} = -D_{yy}\frac{\partial\bar{Q}}{\partial y}\qquad (3.1)$$

where $f = 2\Omega \sin\phi$ is the Coriolis parameter and Q is the quasigeostrophic potential vorticity (the term $K_{yz}\partial Q/\partial z$ is negligible on quasigeostrophic scaling). Thus the momentum budget (3.1) may be regarded as a balance between advection (of mean angular momentum by the residual circulation) and diffusion (of potential vorticity). The basis of the assumption of advection-dominated transport is that if one assumes the stratosphere to be close to nonacceleration conditions such that parcel dispersion is weak—formally $O(\delta)$, say, in some suitable sense where δ is small—then the components of D are also $O(\delta)$, while for the elliptical orbits typical of large-scale atmospheric eddies, L remains $O(1)$. Therefore, the eddy flux is dominated by the $O(1)$ advective component. However, near nonacceleration

conditions this advection serves, to leading order, to cancel the Eulerian mean advection so that the net transport circulation U_T is O(δ). This is clear from (3.1), which tells us that $\bar{v}_*$ and hence also χ_* are O(δ) whence, using (2.18), $\chi_T \sim$ O(δ). Therefore, *both* net advective velocities and diffusivities are formally O(δ), i.e., both effects depend on departures from nonacceleration conditions (Fels et al., 1980; Kurzeja, 1981; Plumb 1982). This argument of course breaks down in equatorial regions, where the quasigeostrophic assumptions on which (3.1) is based becomes invalid. Indeed, in low latitudes a mean meridional circulation can exist even in the limit of vanishing eddy transport; the steady angular momentum budget is then satisfied by the vanishing of the mean angular momentum gradient, rather than of $\bar{v}_*$ (Held and Hou, 1980). However, such a balance is unlikely to obtain away from equatorial regions (and it is a matter of record that it does not) and therefore the formal balance between advection and diffusion should typify the extratropical atmosphere. A careful scaling of the transport equation (2.14) for a vertically stratified constituent confirms that advective and diffusive transport effects are formally of comparable magnitude although, unlike the momentum budget, this is a *global* statement and not necessarily valid locally. Consider, for example, the ratio of diffusive and advective terms in a quasi-horizontal coordinate system defined by the principal axes of D. The vertical advection term is ADV = $-W_T \partial\bar{q}/\partial z$ while, for weak vertical diffusion, the diffusion term is DIFF = $\partial(D_{yy}\partial\bar{q}/\partial y)/\partial y$ whence |DIFF| $\gtrsim D_{yy}|\partial\bar{q}/\partial y|/a$, where a is the earth's radius. Then

$$\left|\frac{\text{DIFF}}{\text{ADV}}\right| \sim \frac{D_{yy}}{|W_T|}\frac{\hat{\gamma}}{a}$$

where $\hat{\gamma} = -(\partial\bar{q}/\partial y)/(\partial\bar{q}/\partial z)$ is the slope of the mean mixing ratio isopleths in this coordinate system. Now, $|W_T| \sim |V_T|H/a$ where H is an atmospheric scale height, and, if we assume $|V_T| \approx |\bar{v}_*|$ (which will become apparent below), $|W_T| \sim |\bar{v}_*|H/a$. But, given that $(\partial\bar{Q}/\partial y)/f \sim a^{-1}$ for realistic flows, (3.1) gives $|\bar{v}_*| \sim D_{yy}/a$. Therefore $|W_T| \sim D_{yy}H/a^2$ whence

$$\left|\frac{\text{DIFF}}{\text{ADV}}\right| \sim \frac{a\hat{\gamma}}{H}.$$

Typically, $a\hat{\gamma}/H$ is of order unity for long-lived tracers, whence diffusive and advective transport are of comparable importance. Indeed, it can be argued (Mahlman, 1985) that the mean isopleth slope of long-lived tracers is determined by just this balance.

The question then arises as to how this statement can be reconciled with the fact that the mean transport of entropy (a quasi-conserved quantity) can be expressed as advection by the residual circulation, without any other transport terms. Under quasi-geostrophic scaling for any constituent whose mean isopleth slope

is sufficiently small (which includes most long-lived stratospheric tracers), (2.14) becomes

$$\frac{\partial\bar{q}}{\partial t} + W_T\frac{\partial\bar{q}}{\partial z} = \bar{s} + \frac{\partial}{\partial y}\left(D_{yy}\frac{\partial\bar{q}}{\partial y} + D_{yz}\frac{\partial\bar{q}}{\partial z}\right). \quad (3.2)$$

If $\partial\bar{q}/\partial z$ is assumed independent of y (cf., the quasi-geostrophic assumption of latitudinally invariant static stability, if q = entropy) then (3.2) may be written

$$\frac{\partial\bar{q}}{\partial t} + \frac{\partial}{\partial y}\left(\tilde{\chi}\frac{\partial\bar{q}}{\partial z}\right) = \bar{s} \quad (3.3)$$

where

$$\tilde{\chi} = \chi_T - D_{yy}\frac{\partial\bar{q}/\partial y}{\partial\bar{q}/\partial z} - D_{yz}. \quad (3.4)$$

Therefore, as a consequence of the quasigeostrophic scaling, the combined effects of advection and diffusion may be represented *mathematically* by an effective circulation $\tilde{\chi}$. This equivalence may become more apparent in the context of Fig. 2. Let $\gamma = (\partial\bar{q}/\partial y)/(\partial\bar{q}/\partial z)$ be the slope of the mixing ratio isopleths. From (2.11)–(2.13), on quasi-geostrophic scaling (when $|D_{zz}| \ll |D_{yy}|$ and $|D_{yz}| \ll |D_{yy}|$) the diffusion may be approximated as linear diffusion along the principal axis making an angle $\alpha \approx D_{yz}/D_{yy}$ with the horizontal. Then (3.4) may be written.

$$\tilde{\chi} = \chi_T + D_{yy}(\gamma - \alpha).$$

Unless $D_{yy} = 0$ or $\gamma = \alpha$ (when the mixing occurs along surfaces of constant $\bar{q}$ and thus achieves no transport of q) $\tilde{\chi} \neq \chi_T$. In the example of Fig. 2 (the $|\alpha| > |\gamma|$) the effect of the diffusion is to reduce the isopleth slopes (by weakening the concentration gradients in the plane of the diffusion); precisely the same effect can be achieved by a circulation as depicted in Fig. 2, whose streamfunction is $D_{yy}(\gamma - \alpha)$ and which appears as the correction to be applied to χ_T in (3.4).

Note, however, that for a passive tracer (3.3) is a purely diagnostic statement, of little predictive value since $\tilde{\chi}$ is a function of isopleth slope and therefore of the solution (and also therefore differs for different
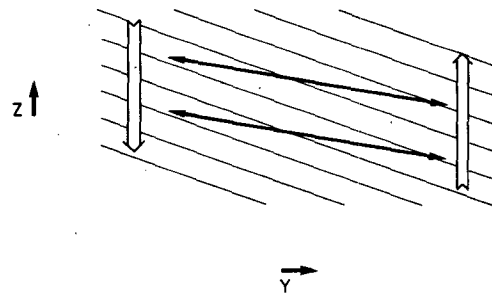

FIG. 2. Illustrating the formal mathematical equivalence of advection and diffusion of a vertically stratified passive tracer under quasi-geostrophic assumptions. Thin lines depict isopleths of $\bar{q}$. Thick arrows show plane of mixing, which tends to reduce the slope of the isopleths. Open arrows depict the sense of the equivalent circulation. See text for discussion.

constituents). It is clear that the description (2.14) in terms of advection and diffusion is the more fundamental and useful one. Setting $q = \theta$ in (3.4), we recover (2.18) with $\chi_* = \tilde{\chi}$, thus identifying the residual circulation as a member of this family. Therefore, even though entropy transport may be described simply by vertical advection by the residual circulation—and indeed this has proved to be a profoundly useful approach to dynamical treatments via transformed Eulerian-mean theory—it should be remembered in the transport context that this "advection" incorporates what we here recognise as diffusive processes of entropy transport.

To return to the calculation of the transport coefficients, it is clear that neither advection nor diffusion may be neglected a priori. One may nevertheless be able to use dynamical insight to place constraints on these coefficients (and thereby reduce the number of variables). The most promising such approach is that of Mahlman et al. (1981) and Tung (1982, 1984) who point out that for almost adiabatic eddies, the diffusion will occur almost along the isentropes. Further, since this implies $K_{yy}\partial\bar{\theta}/\partial y + K_{yz}\partial\bar{\theta}/\partial z \approx 0$, it follows from (2.18) that $\chi_T \approx \chi_*$ (Holton 1981). Therefore, given the residual circulation and mean isentropic slopes (both of which are Eulerian variables, although derivation of the former is still not a trivial exercise for the stratosphere) one is left with the much simpler problem of parameterizing the scalar diffusion rate in isentropic surfaces. However, although these assumptions appear reasonable for most regions of the atmosphere, one can conceive of conditions which violate these assumptions. Mixing processes may be cross-isentropic even for asymptotically small thermal dissipation rates, since the cascade to small scales associated with such events may in fact lead to enhanced dissipation. Vertical, cross-isentropic mixing by internal gravity waves is an example of this effect, which may also be significant for mixing generated by large scale disturbances. Mahlman (1985) discusses the importance of eddy diabatic effects in the transport of constituents relative to isentropic surfaces. In any event we wish to include here calculation of transport rates in the troposphere, where latent heat release and other effects will negate the adiabatic assumption. Therefore, we do not follow this course here.

Instead, the approach adopted in this study is to take the flux-gradient relation (2.5) as the starting point and thence to derive the transport coefficients from a knowledge of eddy fluxes and mean gradients. To derive all four coefficients in this way requires both northward and vertical fluxes of two independent tracers (with nonzero and nonparallel mean gradients). These requirements cannot be met with available atmospheric data, since vertical flux data on a global scale simply do not exist. The required data are, however, readily obtainable from numerical models and we choose to adopt this course, using the GFDL general

circulation/tracer model (hereinafter referred to as "the GCM") to integrate global trace constituent fields forward in time from specified initial conditions and thereby to generate the required eddy statistics. Even so, the selection of these GCM experiments requires care. What we seek to determine is the purely kinematic transport coefficients given by (2.8) and (2.9) which is appropriate for exactly conserved tracers. However, such are effectively ruled out for the purposes of these experiments by the requirement that the two tracers be independent. Although one might choose very different initial conditions for two tracers, the inversion of (2.5) for exactly conserved tracers soon becomes singular when either the gradient of one or other vanishes somewhere (in regions of strong mixing) or when their gradients become parallel, as with time they will (Mahlman and Moxim 1978). Therefore the experiments were conducted with almost-conserved tracers subjected to a weak relaxation to some prescribed distribution $q°(\phi, z)$:

$$\frac{dq}{dt} = -\Lambda(\phi, z)\{q - q°(\phi, z)\} \qquad (3.5)$$

where Λ is chosen to be large enough to maintain nonzero (and nonparallel) gradients, yet sufficiently small that the nonconservative contribution (2.10) to eddy diffusion is small compared to the contribution (2.9) from dispersion—i.e., the relaxation time Λ^{-1} is long compared to the parcel dispersion time scale. The actual choice of $\Lambda(\phi, z)$ and further details of the actual experiments will be discussed in section 4.

One further choice to be made is the time span of the statistics to be used in (2.5). What is aimed for in this GCM approach (and what is usually required in two-dimensional models) is a representation of the seasonal transport characteristics rather than of behavior on shorter time scales. Therefore monthly mean statistics were used in order to give a reasonable resolution of the seasonal cycle without the results being unduly influenced by individual model events. Some calculations were done with different averaging periods to check the stability of the results, as will be discussed below.

4. The GCM experiments

The structure and operation of the GFDL general circulation/tracer model is described by Mahlman and Moxim (1978), to which the reader is referred for details. The model is a finite-difference, sigma coordinate model with horizontal resolution of 265 km and 11 vertical levels at standard mean pressure levels of 990, 940, 835, 685, 500, 315, 190, 110, 65, 38 and 10 mb. The standard height of the top level is thus about 32 km. The tracer experiments are run off-line, i.e., the tracer continuity equation (2.1) is integrated using, in the advection term, six-hourly averaged winds stored every six hours for one year from a previous GCM

TABLE 1. Specifications of tracer experiments.

Experiment	Initial q on Jan 1	Sinks	Duration of experiment (months)
1	ϕ (degrees)	No	6
2	Potential temperature Jan 1	No	6
3	$\sin \phi$	Yes [Eq. (4.1)]	13
4	$-\ln (p/1000$ mb)	Yes [Eq. (4.1)]	13
5	Midlatitude stratospheric distribution—Eq. (6.1)	In troposphere only—Eq. (6.2)	36
6	Zonal-mean field from GCM	At 10 and 38 mb only. Surface source	To equilibrium

experiment; multiyear experiments are run by recycling the wind data. In addition to the advective term, a vertical diffusion, dependent on moist Richardson number, is included to represent subgrid processes (Levy et al., 1982). The model also includes a horizontal diffusion term in which the magnitude of the coefficient depends on the horizontal deformation magnitude and on the relative mixing ratio gradients (Mahlman and Moxim, 1978). Discussion of the model climatology is given in Manabe and Mahlman (1976) and its important characteristics and shortcomings are summarized in Table 1 of Mahlman and Moxim (1978). The most serious shortcomings of the model from a transport perspective are probably deficient eddy kinetic energy in the midlatitude troposphere and, in common with most GCM representations of the stratosphere, an excessively cold polar night stratosphere and absence of major warmings. The former of these probably indicates weak transport in the midlatitude troposphere. The second is probably also indicative of weak transport in the model's winter stratosphere; the implications of this for the model representation of stratospheric tracer transport are discussed by Mahlman et al. (1986). The impact of the poor resolution of the stratosphere, with the uppermost model level being at 10 mb, is difficult to assess, although Mahlman et al. (1986) have discussed some aspects of the impact on vertical transport in the upper levels of the model.

Tracer experiments undertaken in this model have included evolution of an idealised distribution initially similar to the cloud of debris from an atmospheric nuclear bomb test (Mahlman and Moxim, 1978) and simplified ozone (Mahlman et al., 1980; Levy et al., 1985) and N$_2$O experiments (Levy et al., 1982; Mahlman et al., 1986).

Several artificial tracer experiments were run for the present study; these are summarized in Table 1. The first four of these were two pairs of experiments (each pair comprising a horizontally stratified and a vertically stratified tracer) from which the transport coefficients could be determined. The first pair were run for six months from 1 January with exactly conserved tracers whose initial conditions were q set equal to (Experiment 1) latitude (in degrees) and (Experiment 2) potential temperature as specified by the parent GCM on 1 January. These experiments are described in detail in

Mahlman (1985). Monthly mean $\bar{q}$ fields from Experiment 1 for March (shown in Fig. 12a) reveal substantial horizontal mixing in the tropical upper troposphere and subtropical winter stratosphere. In fact, the loss of horizontal mean gradient in the latter region was so severe that attempts to derive the transport coefficients, while successful in January, broke down in February. Therefore, a second set of experiments (3 and 4 in Table 1) were performed. The initial conditions for these runs were even simpler being constant stratifications in the two coordinates y and z, viz. $q_3(\lambda, \phi, z, 0) = \sin\phi$, $q_4(\lambda, \phi, z, 0) = z$. In order to preserve nonzero and nonparallel gradients throughout the course of the experiments, the mixing ratios were relaxed back toward these values according to (3.5). The choice of Λ (which was the same for both experiments) was based on the two requirements discussed in Section 3:

(i) Λ had to be large enough to maintain mean tracer gradients. This criterion was quantified by observing the time scale on which gradients were destroyed in experiments 1 and 2.

(ii) Λ must be small enough not to impact strongly on the eddy transport characteristics. Dispersion rates were estimated from the results of deriving the transport coefficients from experiments 1 and 2, together with velocity covariance statistics, under the assumption that the eddies responsible for transport are quasistationary (this assumption will be justified subsequently).

On this basis a relaxation rate was chosen of the form

$$\Lambda(\phi, p) = a_1(\phi)f_1(p) + a_2(\phi)f_2(p). \qquad (4.1)$$

The $f_1(p)$ and $f_2(p)$ are vertical profiles, piecewise linear in pressure, which describe tropospheric and strato-

TABLE 2. Vertical profiles for the relaxation coefficients in Experiments 3 and 4.

	$f_1(p)$	$f_2(p)$
$p \leq 50$ mb	0	1
50 mb $< p \leq 100$ mb	$\dfrac{p - 50 \text{ mb}}{50 \text{ mb}}$	$\dfrac{100 \text{ mb} - p}{50 \text{ mb}}$
$p > 100$ mb	1	0

spheric relaxation respectively. Their form is given in Table 2. The tropospheric rate coefficient was set at

$$a_1(\phi) = \left[2 + 4 \exp\left(-\frac{\phi^2}{2\delta_1{}^2}\right)\right] \times 10^{-7} \text{s}^{-1} \quad (4.2)$$

where $\delta_1 = 30°$. Because (as will be seen) the location of strongest stratospheric mixing is seasonal, $a_2(\phi)$ was also specified to be so, as follows.

December–March:

$$a_2(\phi) = \left[0.2 + 6.0 \exp\left(-\frac{(\phi - \phi_2)^2}{2\delta_2{}^2}\right)\right] \times 10^{-7} \text{s}^{-1} \quad (4.3a)$$

where $\phi_2 = 20°$ and $\delta_2 = 15°$.

April–June and September–November:

$$a_2(\phi) = \left[0.1 + 2.9 \exp\left(-\frac{\phi^2}{2\delta_2{}^2}\right)\right] \times 10^{-7} \text{s}^{-1} \quad (4.3b)$$

where $\delta_2 = 25°$.

July–August:

$$a_2(\phi) = \left[0.1 + 2.9 \exp\left(-\frac{(\phi - \phi_2)^2}{2\delta_2{}^2}\right)\right] \times 10^{-7} \text{s}^{-1} \quad (4.3c)$$

where $\phi_2 = -30°$ and $\delta_2 = 15°$.

Together, this formulation gives strongest relaxation ($\Lambda^{-1} \sim 20$–40 d) in what were found to be the regions of strongest mixing (tropical troposphere and subtropical winter stratosphere) and much weaker relaxation elsewhere. It was found that this was sufficient to prevent major loss of mean gradients; it will be confirmed a posteriori that its inclusion had little impact on the derived transport coefficients.

Experiments 3 and 4 were run for 13 months from 1 January; the monthly- and zonal-mean mixing ratio fields are shown at three-monthly intervals in Figs. 3 and 4. Despite the relaxation, the mixing ratios in places deviated substantially from their relaxed values, thus revealing the effects of strong transport. Results from Experiment 3 (Fig. 3) shows that the reduction of horizontal gradient occurs most strongly in two regions: the tropical upper troposphere and subtropical winter stratosphere. (The initial gradient, in these regular latitude coordinates, was initially weak at high latitudes.) The vertically stratified tracer of Experiment 4 (Fig. 4) highlights vertical transport processes. The rapid expulsion of gradient from the troposphere reveals the effects of vertical transport there. In the stratosphere the isopleths show a tendency toward the characteristic "poleward-downward" slope of long-lived tracers, with the isopleths being displaced downward in middle and high latitudes of the winter hemisphere and upward in low latitudes of the summer hemisphere.

The eddy fluxes, also shown in Figs. 3 and 4, summarize the eddy component of transport. In middle latitudes the fluxes are directed primarily along the

mean mixing ratio isopleths, rather than across them. This is indicative of advective-type eddy fluxes (antisymmetric **K**) in these regions; indeed this is a characteristic signature of eddy fluxes of conserved tracers in the absence of parcel dispersion (Clark and Rogers, 1978; Plumb, 1979; Matsuno, 1980). In lower latitudes the fluxes are more downgradient, suggestive of diffusive-type eddy transport.

The calculations of **K** (and thence χ_T and **D**) from (2.5) was for the most part straightforward, given the monthly-averaged model results. Because of the differentiation required, some smoothing was inevitable; the components of **K** were evaluated at the midpoint (in ϕ and in z) between adjacent vertical and latitudinal grid points. The model data were interpolated from σ- to p-surfaces prior to the calculation; some problems therefore arose near the bottom boundary where the p-surfaces may intersect the topography. It was found expedient to ignore the 990 mb data altogether; instead of the lowest point for evaluation of K being located midway between the GCM levels at 835 and 940 mb, the results were then interpolated to the midpoint (in z) between 835 and 1000 mb, for reasons that will become apparent in section 6. Even so, σ-to-p interpolation caused problems for the evaluation of eddy fluxes in regions of high topography, especially in the Antarctic and at the latitudes of the Tibetan plateau. In these regions the actual GCM data were ignored and replaced by data interpolated into these regions both in the vertical and horizontal from regions where the data were considered meaningful.

It might perhaps be noted at this stage that these problems in fact indicate a limitation of the zonally-averaged approach at latitudes of high topography. On pressure surfaces that intersect the earth's surface, the zonal mean/eddy separation becomes indistinct (at least without a special formulation of the separation); we do not pursue this issue here.

5. Results

For each of the 13 months of integration of Experiments 3 and 4, the transport tensor **K** was evaluated as outlined in the previous sections. The mean streamfunction χ was also evaluated from the monthly mean $\bar{v}$ by integrating the first of (2.4) in the vertical, given $\chi = 0$ at $p = 0$. The net transport streamfunction χ_T and diffusivity tensor **D** were then determined [following (2.7), (2.8) and (2.16)] by

$$\chi_T = \chi + \frac{1}{2}(K_{zy} - K_{yz}) \quad (5.1)$$

and

$$D = \begin{bmatrix} K_{yy} & \frac{1}{2}(K_{yz} + K_{zy}) \\ \frac{1}{2}(K_{yz} + K_{zy}) & K_{zz} \end{bmatrix}. \quad (5.2)$$

Net transport velocities were then determined from (2.15). Results of this procedure are shown at three-monthly intervals in Figs. 5–8.
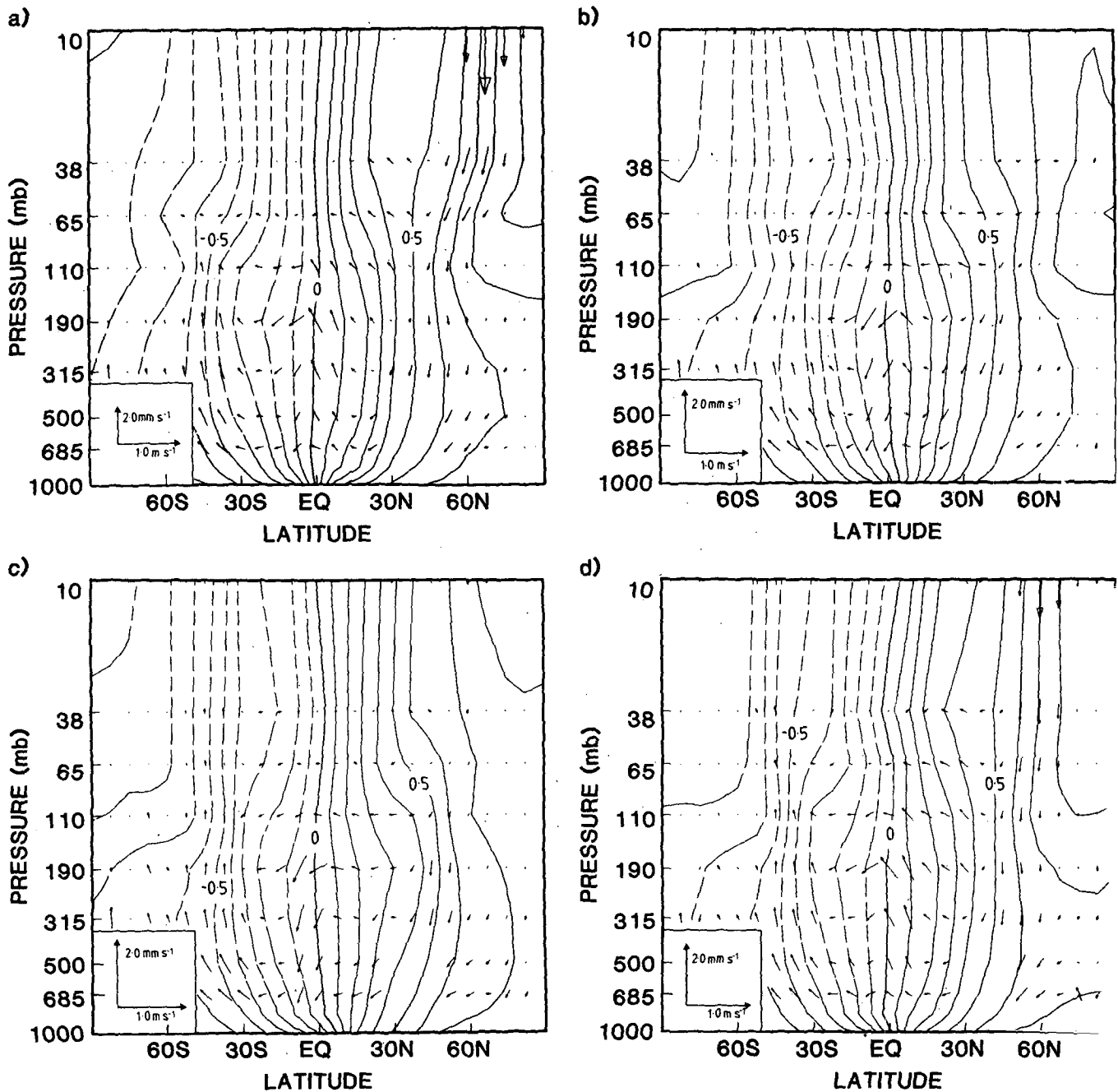
FIG. 3. Evolution of tracer mixing ratio for Experiment 3 for (a) March, (b) June, (c) September and (d) December. Monthly mean of eddy fluxes $(\overline{v'q'}, \overline{w'q'})$ (arrows: scales shown on lower left of each figure) and zonal mean mixing ratio (contours).

The mean meridional circulation $(\overline{v}, \overline{w})$ (Figs. 5a–8a) shows the familiar pattern of low latitude Hadley cells in the troposphere and Ferrel cells in middle tropospheric latitudes, penetrating up through the stratosphere in the winter hemisphere (and, more weakly, in the Northern Hemisphere during spring and autumn). A summer-to-winter circulation is also evident in the model stratosphere near the solstices. These Ferrel cells are not, however, apparent in the transport circulation U_T (Figs. 5b–8b), which is dominated by two Hadley cells throughout the year in the troposphere and a single cell in the stratosphere from the low latitude summer hemisphere to middle and high latitudes of the winter hemisphere. This is in accord with theoretical expectation, given that U_T is related to the residual and Lagrangian-mean circulations, and as such the successful cancellation of the Ferrel cell lends credibility to the calculation. In fact, the structure of U_T is

a)

b)

c)

d)
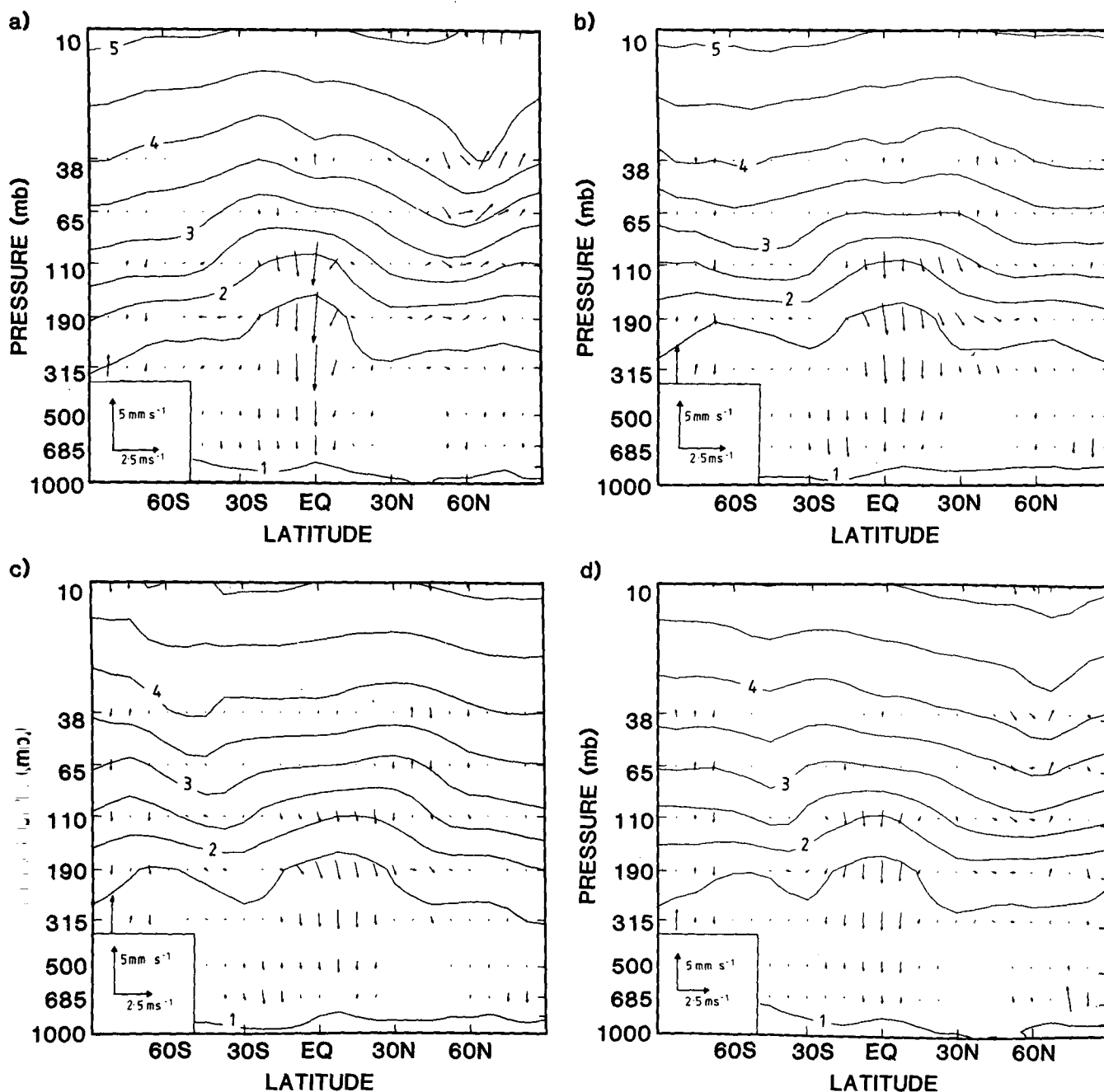
FIG. 4. As in Fig. 1 but for Experiment 4.

much simpler than that of the residual circulation; the latter is shown for January in Fig. 9a. Comparing this with Fig. 5b, it can be seen that the two circulations are quite similar in the stratosphere but that U_T is much the simpler of the two in the troposphere, where the residual circulation is characterized by a tropical Hadley cell and a direct cell in the high latitudes of each hemisphere. These features of the residual circulation are also apparent in atmospheric circulation data (Edmon et al., 1980).

The Lagrangian-mean velocity $\bar{u}^L = (\bar{v}^L, \bar{w}^L)$ was also determined, according to the relation

$$
\left.\begin{array}{c} \bar{v}^L \cos\phi \\ \bar{w}^L \end{array}\right\} = \begin{cases} V_T \cos\phi + \dfrac{\partial}{\partial y} D_{yy} + \dfrac{1}{p}\dfrac{\partial}{\partial z}(pD_{yz}) \\[2mm] W_T + \dfrac{\partial}{\partial y} D_{yz} + \dfrac{1}{p}\dfrac{\partial}{\partial z}(pD_{zz}). \end{cases} \tag{5.3}
$$

It can easily be shown, given (2.14) that $\bar{u}^L$ thus defined is the velocity of the center of mass of a narrow tube
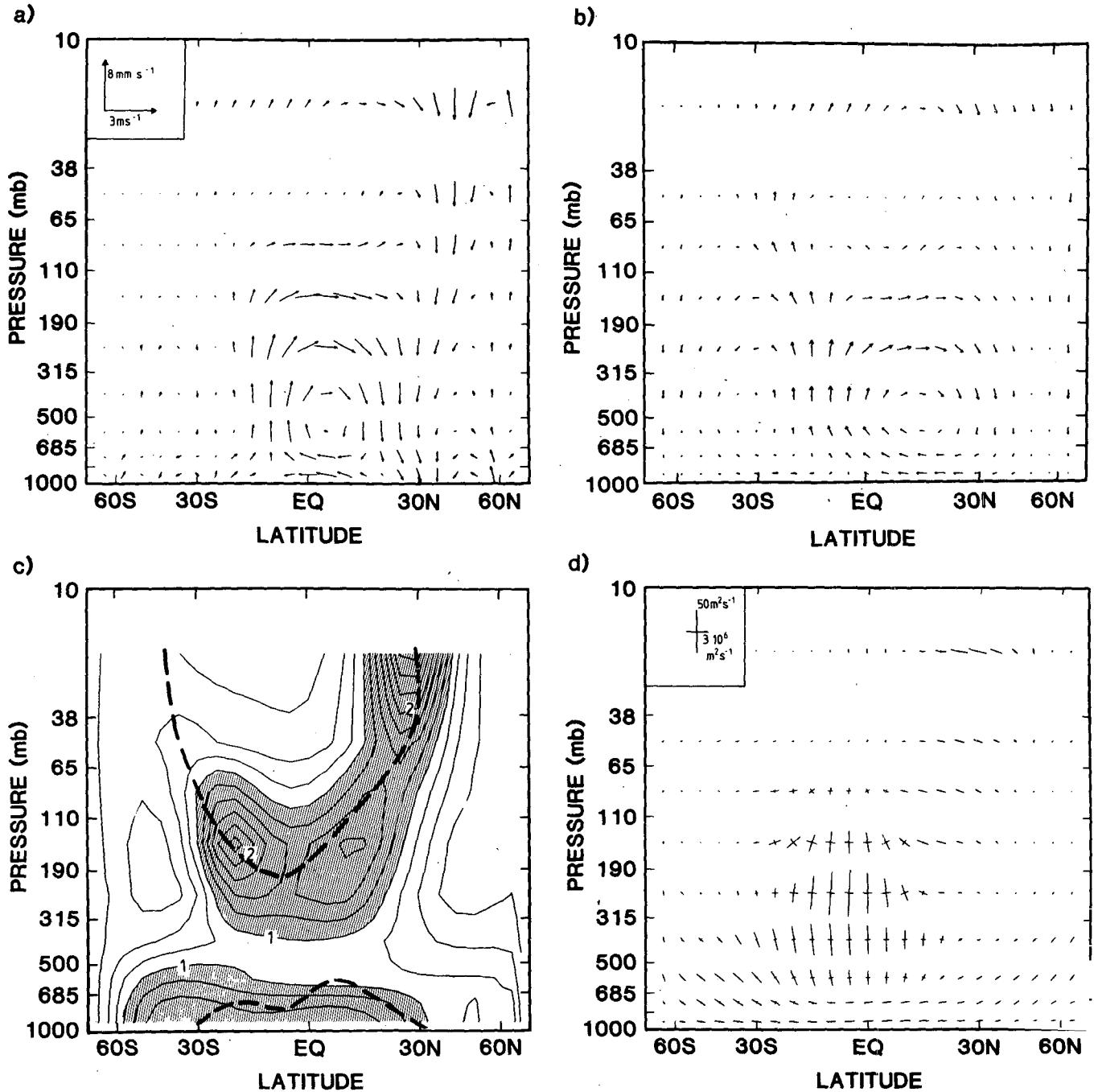
FIG. 5. Derived transport characteristics for January from GCM results of Experiments 3 and 4. (a) Mean circulation ($\bar{v}$, $\bar{w}$) and (b) Net circulation (V_T, W_T); scales for both (a) and (b) are shown at upper left of (a). (c) D_{yy} (10^6 m^2 s^{-1}). Dashed lines follow axis of zero zonal wind . (d) Diffusivity tensor D plotted relative to its local principal axes. Scale shown at upper left. Note that in (a), (b) and (d) the relative vertical horizontal scales are chosen such that the directions shown are meaningful as plotted.

of conserved tracer. For small amplitude eddies, $\bar{u}^L$ reduces to the expression of Andrews and McIntyre (1978) for $\bar{u}^L$ in terms of parcel displacement statistics, given (2.9) [see Eq. (31) of Plumb (1979)]. As noted earlier, $\bar{u}^L$ is not in general a nondivergent velocity unless the diffusivities are spatially homogeneous. In fact,

(5.3) reveals a tendency, in addition to the term U_T, for the Lagrangian-mean flow to be directed towards a region of maximum diffusivity. Andrews and McIntyre (1978) noted this effect and illustrated it with the example of $\bar{u}^L$ being directed away from a smooth wall in the presence of parcel dispersion. These char-
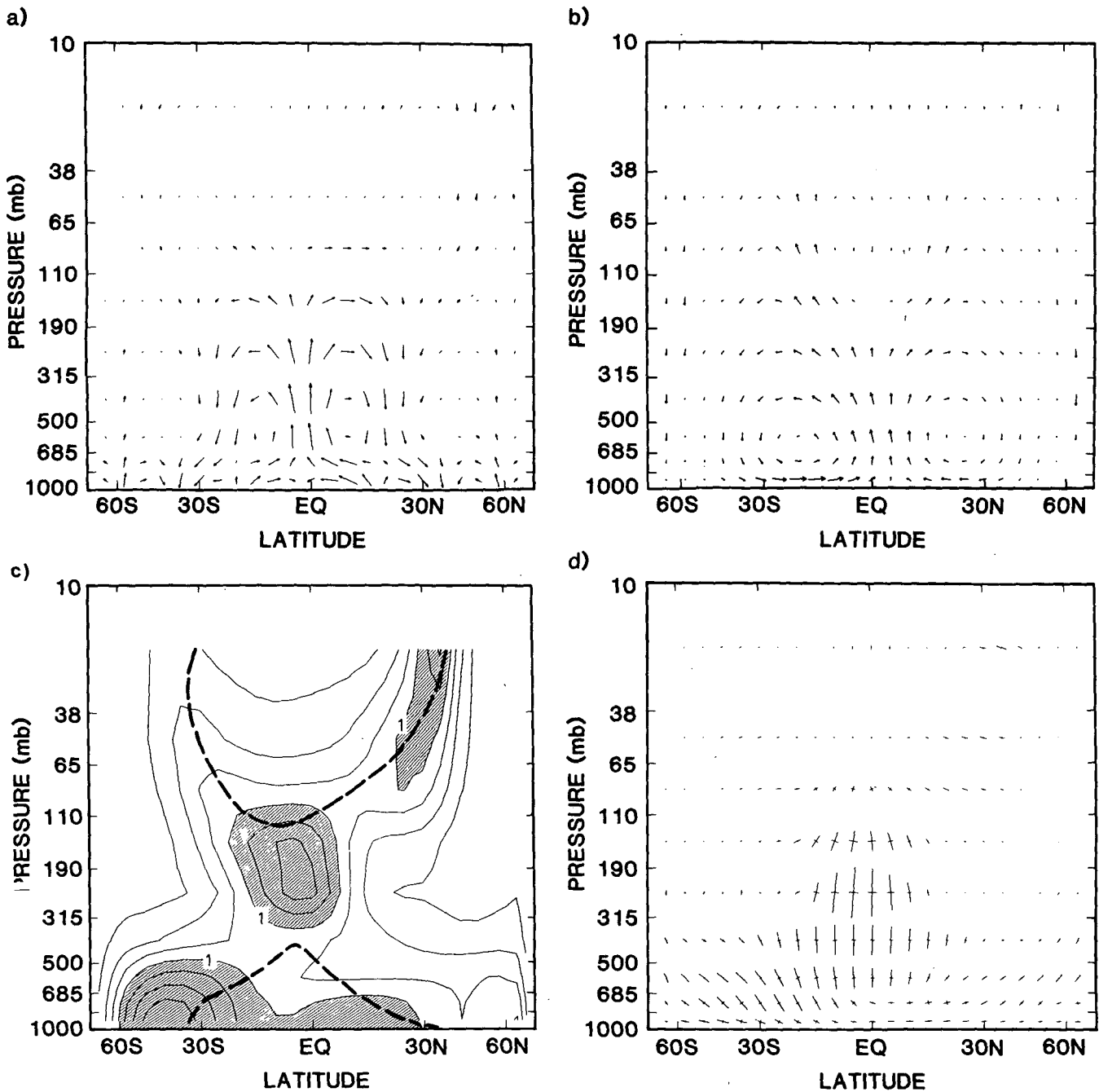
a)

b)

c)

d)

FIG. 6. As in Fig. 5 but for April.

acteristics are evident in the January Lagrangian-mean circulation shown in Fig. 9b, especially in the tropical troposphere, where this flow is directed into the strong vertical mixing region in mid-troposphere. There is, however, some overall similarity with U_T and $\bar{u}_*$ in the stratosphere.

The calculated horizontal eddy diffusivities D_{yy} are shown in Figs. 5c–8c. In accord with theoretical ex-

pectation, this quantity is found to be positive almost everywhere, with small negative values occurring only where the neighboring values are small (usually near the poles). Large values (1–2×10^6 m^2 s^{-1}) occur in the lower troposphere, apparently indicating mixing by synoptic eddies. The result that this mixing is stronger in middle latitudes of the Southern Hemisphere than in the Northern Hemisphere is consistent with
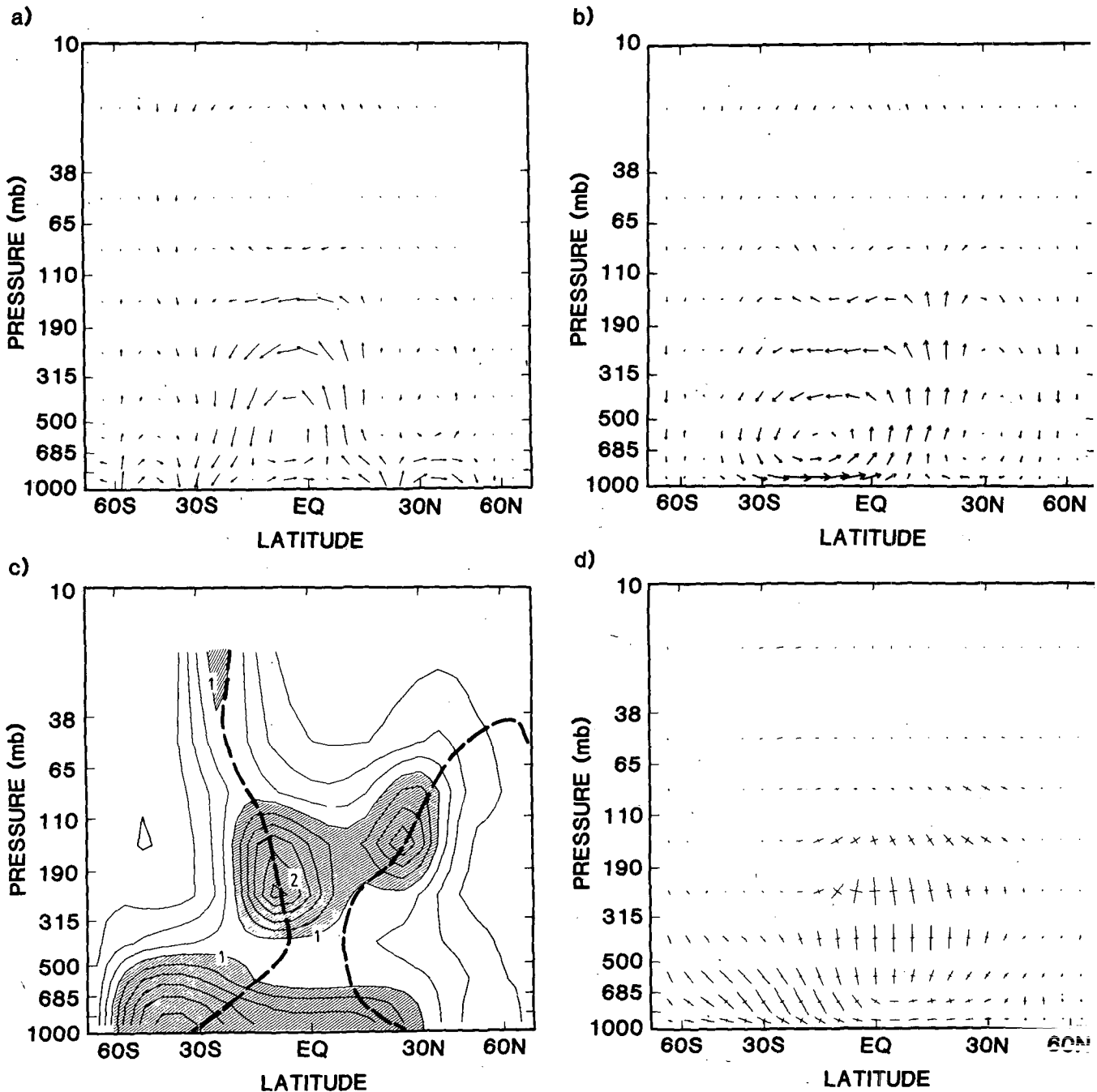
a)

b)

c)

d)

FIG. 7. As in Fig. 5 but for July.

the fact that the transient eddy kinetic energy is larger in the model southern hemisphere throughout most of the year (Manabe et al., 1974). The dominant feature, however, is a band of strong horizontal mixing stretching across the tropical upper troposphere and upward into the subtropics of the winter stratosphere (weakly into the subtropics of both hemispheres around the equinoxes). Indeed in January the strongest mixing

anywhere in the model atmosphere (as measured by the magnitude of D_{yy}) is to be found in the subtropical winter stratosphere. The detailed kinematics of this mixing are described by Mahlman (1985) for Experiment 1. The January-mean flow at these levels, which is shown for 10 mb in Fig. 4.2 of Mahlman and Moxim (1978), is dominated by the Aleutian anticyclone over the North Pacific ocean. Mahlman (1985) described
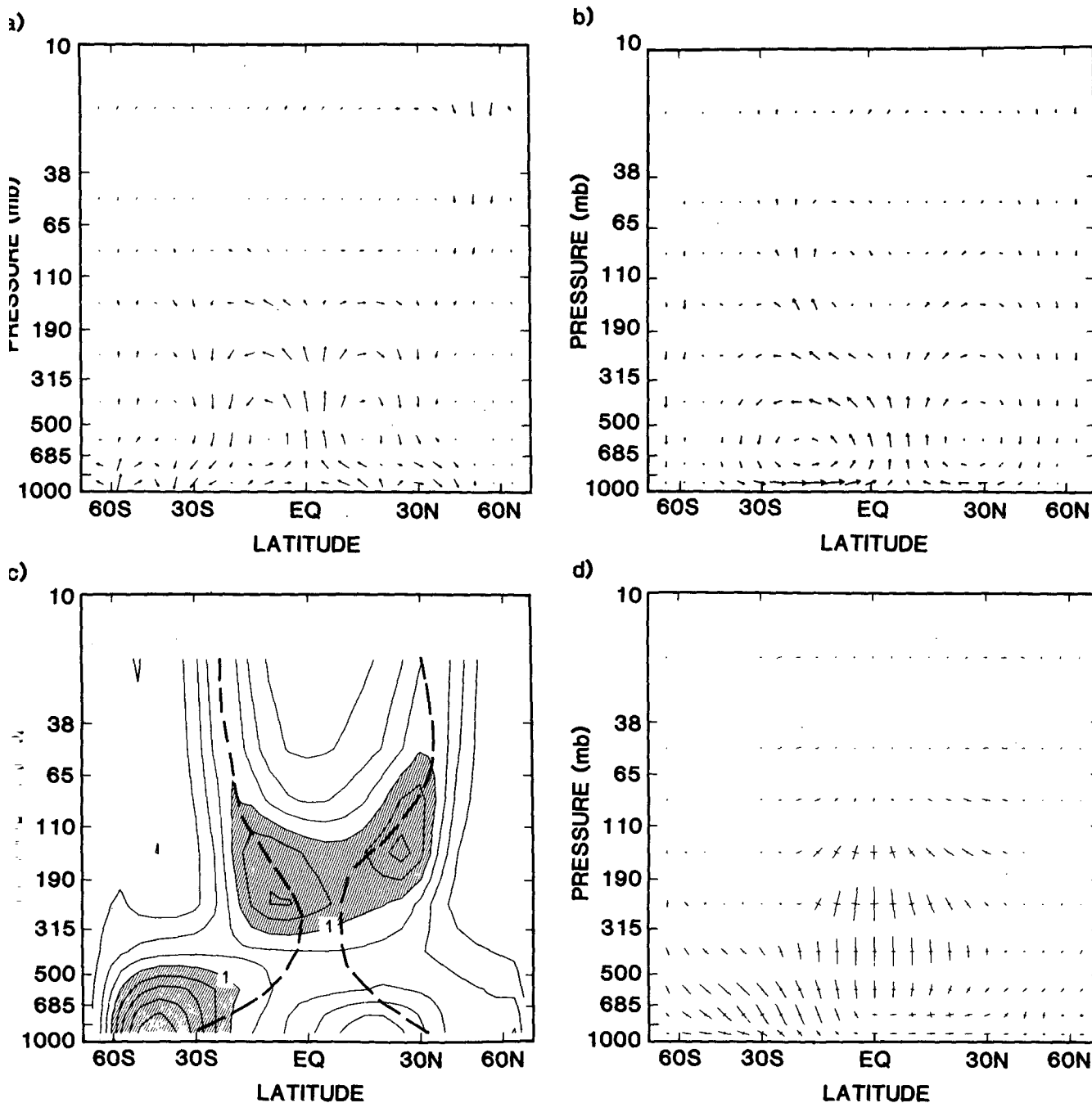
a)

b)

c)

d)

FIG. 8. As in Fig. 5 but for October.

the evolution of q on the 480 K isentropic surface during the first 11 days of the experiment. Attention is drawn in his Fig. 4 to two ribbons of tracer initially (Jan. 1) located in the bands $18°-24°N$ and $48°-54°N$. As early as two days later these ribbons are severely contorted, stretched and displaced latitudinally in the region over the North Pacific and the United States. It is clear that this behavior is associated with regions of

strong deformation on the southeastern and southwestern flanks of the Aleutian anticyclone. Two days later these ribbons have folded and portions have actually broken off—having been stretched to such an extent that the GCM subgrid diffusion has become important. Thus, in only four days, the latitudinal gradient of q is weakened and, in places, actually reversed over much of the Pacific/North American region between
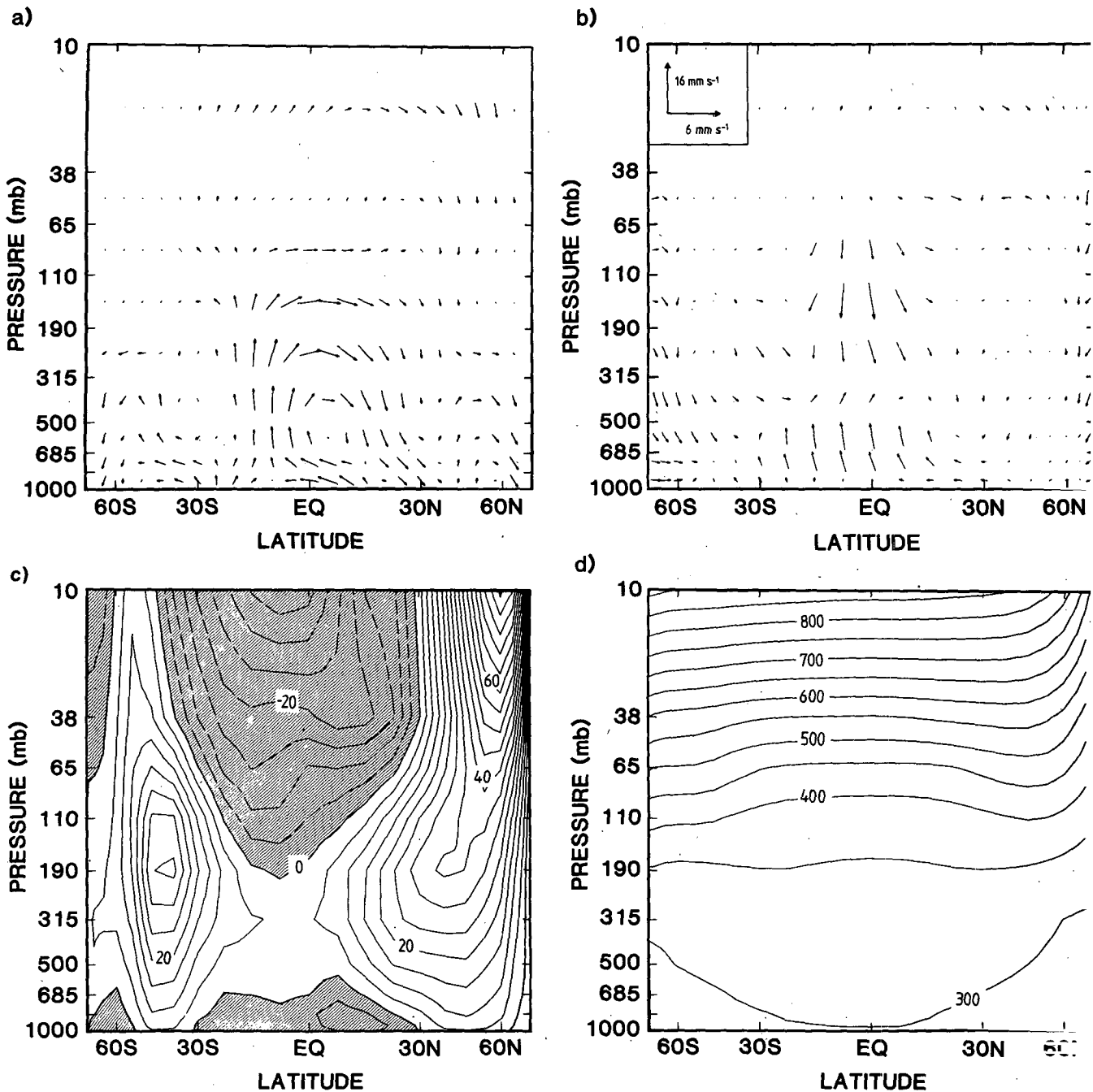
FIG. 9. Further monthly mean characteristics of GCM for January. (a) Residual mean circulation (v_*, w_*). Scale as for Fig. 5a. (b) Lagrangian----circulation defined by (5.3). Scale shown at upper left. (c) Mean zonal wind (m s^{-1}). (d) Mean potential temperature (K).

about 20–40°N. Mahlman (1985) also draws attention to similar, if weaker, mixing events occurring in the midlatitudes of the Southern (summer) stratosphere apparently associated with migrating cyclonic disturbances; this is also evident in a local maximum in D_{yy} (Fig. 5c).

There seems little doubt that the mixing in the Northern subtropics is a manifestation in the GCM of

the breaking of quasi-stationary planetary waves identified by McIntyre and Palmer (1983, 1984) on the basis of the evolution of Ertel potential vorticity (a dynamical tracer) in the stratosphere during February 1979 (see also Clough et al., 1985). This quantity exhibited behaviour very similar to that described here, with ribbons of high potential vorticity becoming stretched out on the southern flank of the Aleutian

anticyclone. Similar behaviour has been identified in LIMS-derived maps of ozone during the same period (Leovy et al., 1985). As McIntyre and Palmer (1983, 1984) and Mahlman (1985) have emphasized, it is the formation of closed eddies in the weak low-latitude winds that is crucial to the dispersion of tracers; at high northern latitudes in the GCM [see Fig. 4.2 of Mahlman and Moxim (1978)] the flow is wavy but essentially laminar and therefore parcel dispersion is weak, even though the Eulerian eddy amplitudes maximize there. (This serves to exemplify the crucial distinction, noted in section 2, between Eulerian and Lagrangian eddy statistics). It is, therefore, to be expected that mixing arising from quasistationary waves will concentrate in regions of weak zonal wind. The mean zonal wind for January in the GCM is shown in Fig. 9c; by comparison with Fig. 5c it can be seen that the entire band of mixing in the winter stratosphere and tropical upper troposphere coincides with the band of weak zonal winds between the equatorial easterlies and midlatitude westerlies. Indeed the band of maximum mixing closely follows the migration of the $\bar{u} = 0$ line, shown dashed of Figs. 5c–8c, throughout the year. Conversely, note from Figs. 5c and 9c that the mixing is particularly weak in regions of strong zonal wind.

The elevated band of strong mixing thus appears to be sustained by eddies propagating upward and equatorward from the midlatitude lower troposphere (cf., Edmon et al. 1980) and breaking in the weak winds of the tropical upper troposphere and subtropical winter stratosphere. In the winter stratosphere, we have seen that the quasistationary eddies are dominant. Even in the upper troposphere and summer stratosphere, the close association with the zero wind line suggests a strong link with quasistationary waves. However transient disturbances might also be expected to break where the winds become small (relative to the eddy phase velocity). Because of the strong shear in the upper troposphere and the finite spatial extent of the band of mixing, the band is also reasonably well mapped out by isotachs of $|\bar{u}|$ up to about 15 m s^{-1}. It seems probable (Mahlman, 1985; Mahlman et al., 1986) that transient eddies are also contributing to the mixing here, especially since, over the year, the mixing in the southern subtropics is more intense than in the northern subtropics and the stationary eddies are rather weak in the Southern Hemisphere. Certainly, in the real world, there are strong indications that transient eddy effects are more important than stationary eddies in this region; from the quasigeostrophic relation

$$\frac{1}{p} \nabla \cdot \mathbf{F} = \overline{v'Q'} \cos\phi \qquad (5.4)$$

(e.g., Edmon et al. 1980), where $\mathbf{F}$ is the quasigeostrophic Eliassen–Palm flux, and using (3.1), it follows that the local ratio of transient-to-stationary eddy-induced mixing can be estimated from the ratio of their respective Eliassen-Palm flux divergences. In the

Northern subtropics in winter, the transient eddy divergence is larger than that due to the stationary eddies (Edmon et al. 1980; their Figs. 4 and 5).

Other components of the diffusion tensor are consistent with dynamical reasoning. Figs. 5d–8d show all components of the tensor, locally rotated and plotted relative to its principal axes according to (2.11) and (2.12). The significance of the plotting format in the figures is that the crossed lines mark the major and minor axes of an ellipse which has the same shape as the isopleths of a tracer diffusing from an initial point source at the centre of the cross. The regions of large D_{yy} are evident in the quasi-horizontal component of the tensor; the influence of D_{yz} manifests itself as a tilting of the principal axis from the horizontal. Outside the tropics, D_{zz} is small and the diffusion occurs almost entirely along a single axis, tilted at an angle $\frac{1}{2} \tan^{-1} (2D_{yz}/D_{yy}) \approx D_{yz}/D_{yy}$ to the horizontal [cf., (2.11)]. As noted in section 3, if the eddies are adiabatic and the mean isentropes are steady, diffusion should be directed along the mean isentropes. These surfaces are shown for January in Fig. 9d; a comparison with Fig. 5d makes it clear that qualitatively this relationship is obeyed outside the tropics, in both troposphere and stratosphere, although there is a systematic tendency for the mixing surfaces to slope more steeply than the isentropes (consistent with the arguments of Mahlman, 1985).

Following the discussion in section 3, this result explains the similarity between the transport and residual circulations in the model stratosphere. However, the diffusion also appears to be quasi-adiabatic in the model midlatitude troposphere, where the two circulations are quite different. This difference must arise either because of a breakdown of the validity of the quasigeostrophic representation of the entropy budget [and the vertical eddy heat fluxes may indeed be larger than a quasigeostrophic scaling would have us believe—cf., Simmons and Hoskins, 1978; Edmon et al., 1980] or because of significant latent heat release, in which case the transport coefficients derived here may not be applicable to entropy transport.

The other dominating feature of Figs. 5d–8d is the large vertical diffusivity in the tropical troposphere. This becomes as large as 60 m^2 s^{-1} in the upper troposphere, corresponding to a time scale for mixing through the depth of the tropical troposphere of around 40 days—shorter than most time scales of interest in global transport problems. It should be emphasized here that these values for $\mathbf{D}$ are the diffusion rates directly associated with the eddy fluxes of resolved motions; the transport properties of the subgrid parameterized mixing will be discussed below. Outside the tropical troposphere, the values of D_{zz} due to resolved model motions were smaller (<10 m^2 s^{-1} in the troposphere, $\leqslant 0.4$ m^2 s^{-1} in the stratosphere) and apparently not well determined, the calculated values being negative in some places and generally not well struc-

tured. The reason for this appears to be that the determination of D_{zz}, via the relation

$$D_{zz} = K_{zz} = \frac{\left[\overline{w'q_1'}\frac{\partial \bar{q}_2}{\partial z} - \overline{w'q_2'}\frac{\partial \bar{q}_1}{\partial z}\right]}{\left[\frac{\partial \bar{q}_1}{\partial y}\frac{\partial \bar{q}_2}{\partial z} - \frac{\partial \bar{q}_2}{\partial y}\frac{\partial \bar{q}_1}{\partial z}\right]} \qquad (5.5)$$

is ill-conditioned in regions where the vertical eddy fluxes are dominated by the advective contribution. Fortunately even the larger values of D_{zz} in the stratosphere are small enough that vertical diffusion is negligible there for mature, long-lived tracers.

In addition to the transport accomplished by the macroscopic model-resolved eddies is the contribution from the parameterized subgrid processes. These were assimilated into the present formalism by calculating the zonally-averaged fluxes associated with these components of the transport and again calculating equivalent diffusion coefficients. In fact, the small-scale horizontal fluxes were found to be everywhere and at all times much smaller (by several orders of magnitude) than the horizontal macroscale fluxes, and so no correction to D_{yy} or D_{yz} is required. (That does not mean, of course, that the subgrid mixing processes are unimportant since, as noted earlier, they may be influential in fixing the large-scale fluxes). Vertical transport by the parameterized subgrid motions was, on the contrary, far from negligible in the troposphere. Derived values of $D_{zz}^{(s)}$, the effective vertical diffusion coefficient for the subgrid transport, are shown in Fig. 10. Rather suprisingly, this mixing maximizes in middle latitudes (and in summer) rather than in the tropics; while there is a local maximum in the region of the ITCZ its intensity is almost a factor of 10 less than that of the explicit eddy transport in this region (though it may be that these resolved motions are triggered off by the moist Richardson number-dependent parameterized mixing events). In midlatitudes $D_{zz}^{(s)}$ is typically 10 m² s⁻¹ and is thus comparable with or larger than the vertical diffusivity associated with the macroscopic motions in the model.

A few tests were made to check the derivation procedure. The first of these relates to the use of monthly mean statistics. The smooth month-to-month variation found in the results confirms their stability. This aspect was checked further by compiling the statistics half-monthly and repeating the calculation for the first few months of the year; the differences thus found in the derived coefficients were small, except for the first half-month period for which the calculated diffusivities were somewhat larger than the January means. This is presumably due to the initialization of the experiments with longitudinally constant mixing ratio. Very rapidly the mixing ratio isopleths would be distorted approximately into the configuration of the model streamlines. This transient initialization effect would manifest itself as a mixing in the zonal mean (cf., Fig. 2 of Plumb

1979) but is of course quite different from the sustained parcel dispersion discussed previously. In order to assess whether this behavior renders the January results unrepresentative, the calculation was repeated for the 13th month of integration, i.e., the second January. The advecting velocities used in the GCM were exactly the same as those for the first January but the tracer field at the beginning of the second year was rather different, being a mature field (the relaxation being too weak to have much impact on the longitudinal variability). Results are illustrated by the D_{yy} field for the second January, shown in Fig. 11a. Comparison with Fig. 5c confirms the repeatability of the results.

Another aspect tested was the impact of the imposed relaxation on the derived coefficients. Figure 11b shows D_{yy} calculated for January from the results of Experiments 1 and 2, which included no relaxation (recall that the determination of K from these experiments did not break down until February). While the calculated diffusivities in the presence of relaxation (Fig. 5c) are, as might be expected from the discussion of section 2, a little larger than those of Fig. 11b, differences are everywhere small (mostly less than 10 percent).

6. A zonally averaged model and comparison with the GCM

The calculation of GCM-based transport coefficients affords an unprecedented opportunity to assess the validity of the flux-gradient relation (2.5) as a basis for the parameterization of global transport of trace constituents. This was done by implementing the parameterization in a two-dimensional (zonally averaged) model (hereinafter "the 2D model"), using the derived transport coefficients χ_T and D on a month-by-month basis in the integration of (2.14) and comparing the evolution of tracer mixing ratios in experiments with this model with the zonally-averaged evolution of parallel experiments in the parent GCM. In order to make the comparison meaningful, the 2D model was designed to be as similar as possible to the GCM in all respects except (of course) longitudinal resolution. Therefore, the vertical and latitudinal structure of the 2D model was chosen to be almost identical to that of the GCM, the exceptions being that the former was defined in pressure, rather than sigma, coordinates and that the lowest two levels (at $\sigma = 0.940$ and 0.990) of the GCM were replaced by a single level (1000 mb) in the 2D model. (As discussed in section 4, the transport coefficients could not be properly evaluated in the lowest GCM layer.) The finite difference scheme adopted was based on that used in the GCM but, because the derivation of the transport coefficients necessarily involved some spatial smoothing (in order to evaluate fluxes and gradients at the same locations), the two could not be made exactly compatible. Finally, in order to focus attention on the parameterization of the transport terms only, the comparison between the two
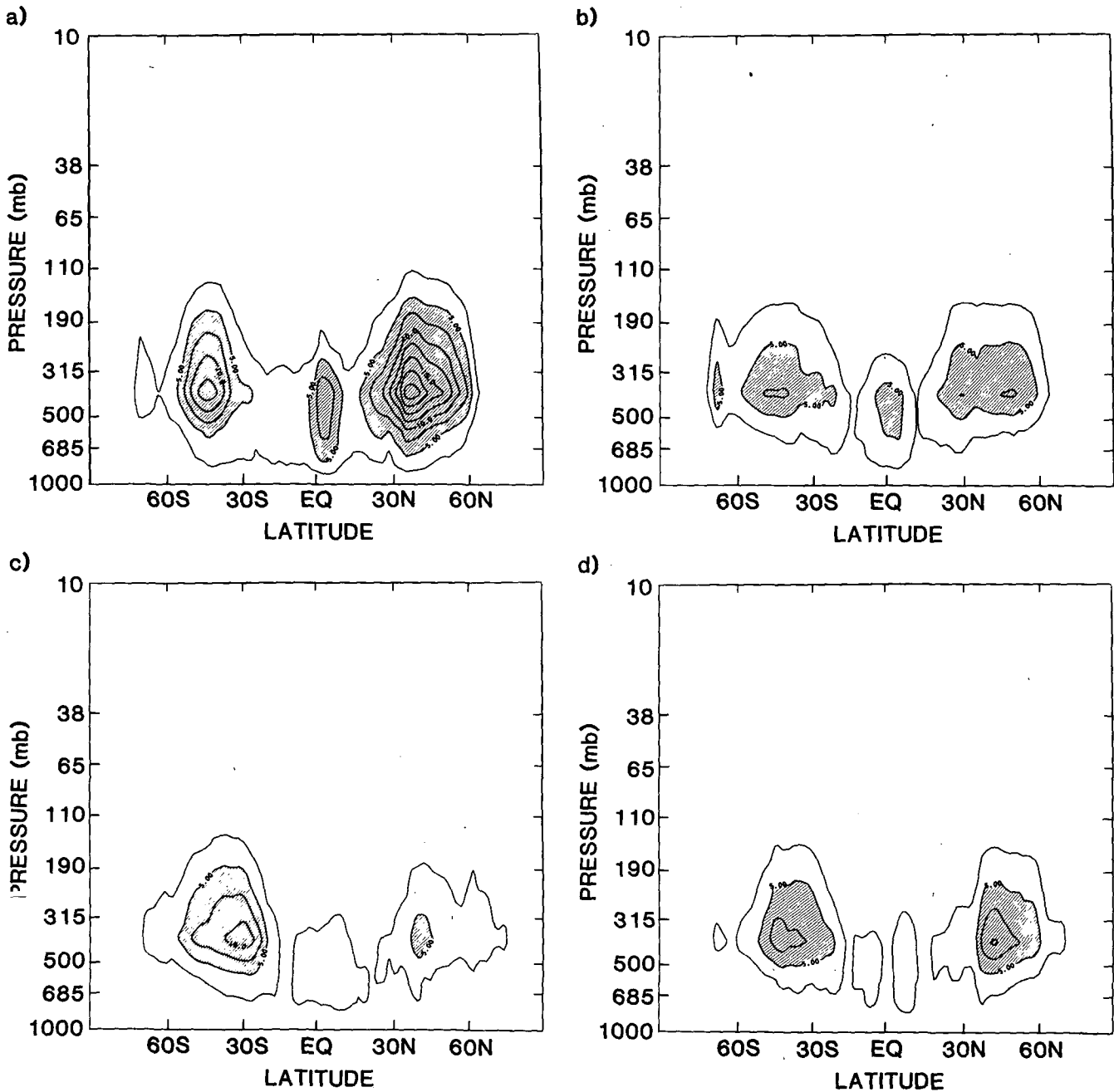
FIG. 10. Vertical diffusivities $D_{zz}^{(q)}$ (m^2 s^{-1}) associated with parameterized subgrid transport in the GCM. Monthly mean fields for (a) January, (b) April, (c) July and (d) October. Contour interval 2.5 m^2 s^{-1}; values greater than 5 m^2 s^{-1} are shaded.

models was based on artificial tracer experiments for which the source or sinks in the GCM could be expressed in the form $s = S - \Lambda q$ where S and Λ may be functions of latitude and height but are independent of longitude (and therefore also independent of longitudinally-dependent model variables such as temperature or rainfall). Then $\bar{s} = S - \Lambda \bar{q}$ exactly and any ambiguities arising from the parameterization of $\bar{s}$ in terms of eddy quantities (e.g., Tuck, 1979) were thus avoided.

The diffusivities used in this model were the sum of those obtained for the resolved eddy transport and the subgrid vertical mixing. As noted in section 5, the derived diffusion rates were in some places small and negative. These values could not of course be used in the 2D model without generating instabilities. Therefore some quality control was exercised on **D**, specifically to satisfy conditions (2.14); this was done by setting D_{yy} and D_{zz} to minimum values [$1.0 \times 10^4 \cos^2\phi$ m^2 s^{-1} for D_{yy} and 0.1 m^2 s^{-1} (stratosphere) or 1 m^2
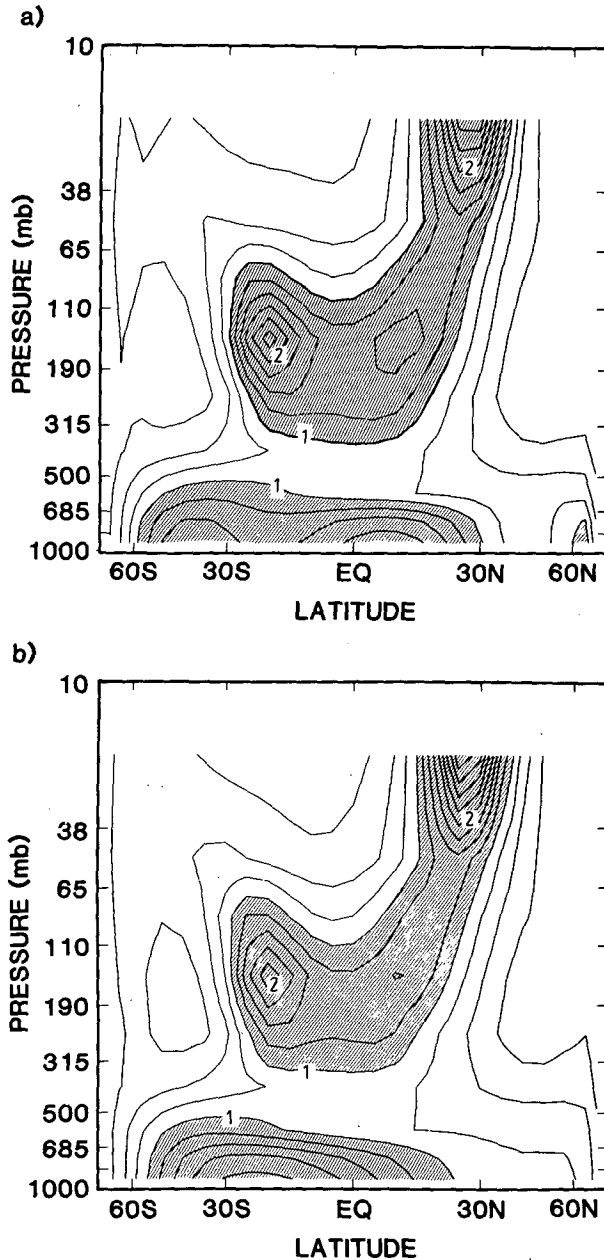
a)

b)

FIG. 11. Illustrations of the stability of the derived transport coefficients. D_{yy} (10^6 m^2 s^{-1}). (a) Derived from the second January (month 13) of Experiments 3 and 4. (b) Derived from January of Experiments 1 and 2.

s^{-1} (troposphere) for D_{zz}] wherever the calculated values were less than these. Because D_{zz} was considered to be the most poorly determined of the coefficients, at any grid points not satisfying the criterion $D_{yz}^2 \leqslant D_{yy}D_{zz}$ after this procedure, D_{zz} was set equal to D_{yz}^2/D_{yy}. The proportion of coefficients requiring such modification was small and, even after these increases, the modified values were almost everywhere too small to give significant contributions to large-scale transport.

The comparisons were based on Experiments 1, 2, 5 and 6 of Table 1. The GCM runs of the first two of these have already been described in Section 5 and in Mahlman (1985); results from the 2D model are compared with the GCM results in Figs. 12 and 13. Overall, agreement is good, although there is some evidence that the 2D model fails to reproduce some of the smaller-scale detail of the GCM results, and some more serious shortcomings are apparent. Figure 12 compares the model results for Experiment 1 for March and June. The predominant stratospheric feature—the destruction of the latitudinal gradient of q in the winter subtropics—has been reproduced very well in the 2D model; indeed the overall representation of the stratospheric evolution is good, although the 2D model underpredicts the retention of high q values in high latitudes of the winter lower stratosphere. The loss of structure in the troposphere is also reasonably well represented by the 2D model results but at a slightly slower rate than in the GCM run. Perhaps not surprisingly, it was found that if the contribution $D_{zz}^{(s)}$ to vertical diffusion associated with the subgrid processes was omitted, the 2D model rapidly generates and maintains strong and unrealistic vertical gradients in the troposphere.

Results from Experiment 2 are compared in Fig. 13. This experiment was initialized with q equal to potential temperature on 1 January of the parent GCM; this initial condition is not shown here but the zonal average of the initial field is in fact very similar to the January mean $\bar{\theta}$ shown in Fig. 7d. Because the weak tropospheric vertical gradient of q rapidly becomes yet weaker during the course of the integration, the comparison between the two models is essentially a test of the ability of the 2D models to predict the evolution of a vertically stratified stratospheric tracer. In fact, as can be seen from Fig. 13, the comparison is good. Again, the structure of the 2D model results lacks some of the finer detail of the GCM results (e.g., the low latitude minimum of q is less sharp in the former) but the poleward-downward slopes of the tracer isopleths are well reproduced, especially in the lower stratosphere. The slopes are, however, a little weak in midlatitudes of the uppermost model layer. This may appear to indicate excessive horizontal diffusion in the 2D model; however, in experiments with the model in which the value of D_{yy} was reduced, the overall agreement was found to deteriorate rather than improve. Furthermore, reduction of D_{yy} was found to produce a marked deterioration in the 2D model results of Experiment 1, so it seems unlikely that the horizontal diffusion is excessive. In further experiments, it was found that the isopleth slopes are sensitive to changes in χ_T (in accord with the conventional view that these slopes represent a balance between the steepening influence of advection and flattening by quasi-horizontal diffusion). It is therefore possible that errors in the derivation of χ_T, arising from vertical smoothing in the
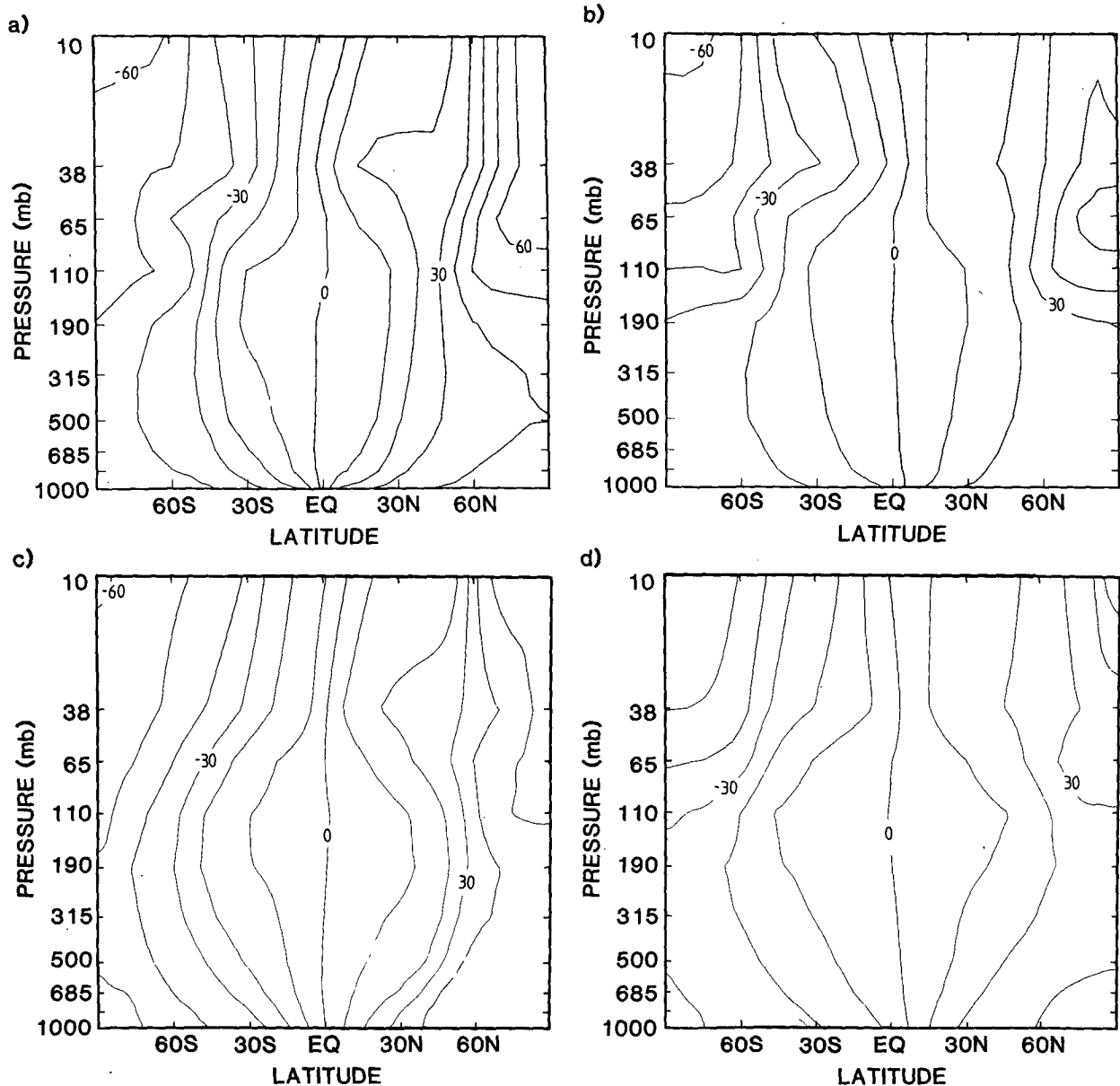
FIG. 12. Comparison of GCM and 2D model results for Experiment 1. Monthly mean mixing ratios.
Zonal mean GCM results for (a) March and (b) June; 2D model results for (c) March and (d) June.

uppermost layer (where the vertical resolution is poor) are responsible for an underestimate of χ_T there.

Despite the shortcomings noted above, the overall conclusion from these two experiments is that the eddy flux parameterization has proved to be relatively successful. However, since these two experiments were in fact similar to those (experiments 3 and 4) from which the coefficients were determined, it seems desirable to extend the comparison to other experiments which might more properly be regarded as independent.

The first of these (Experiment 5 of Table 1) is a variation of the case studied by Mahlman and Moxim (1978) as an idealized study of the evolution of the

stratospheric debris from atmospheric nuclear bomb tests. The differences between Experiment 5 and that of Mahlman and Moxim were designed to meet the criteria specified above to ensure that the loss of longitudinal resolution in the 2D model was the only major difference between this model and the GCM. The initial condition on 1 January (Yr 1) was taken to be a *zonally uniform* distribution

$$q(\lambda, \phi, z) = 1000 \exp\left(\frac{-(z - z_0)^2}{2\Delta z^2}\right) \exp\left(\frac{-(\phi - \phi_0)^2}{2\Delta\phi^2}\right)$$

$$(6.1)$$

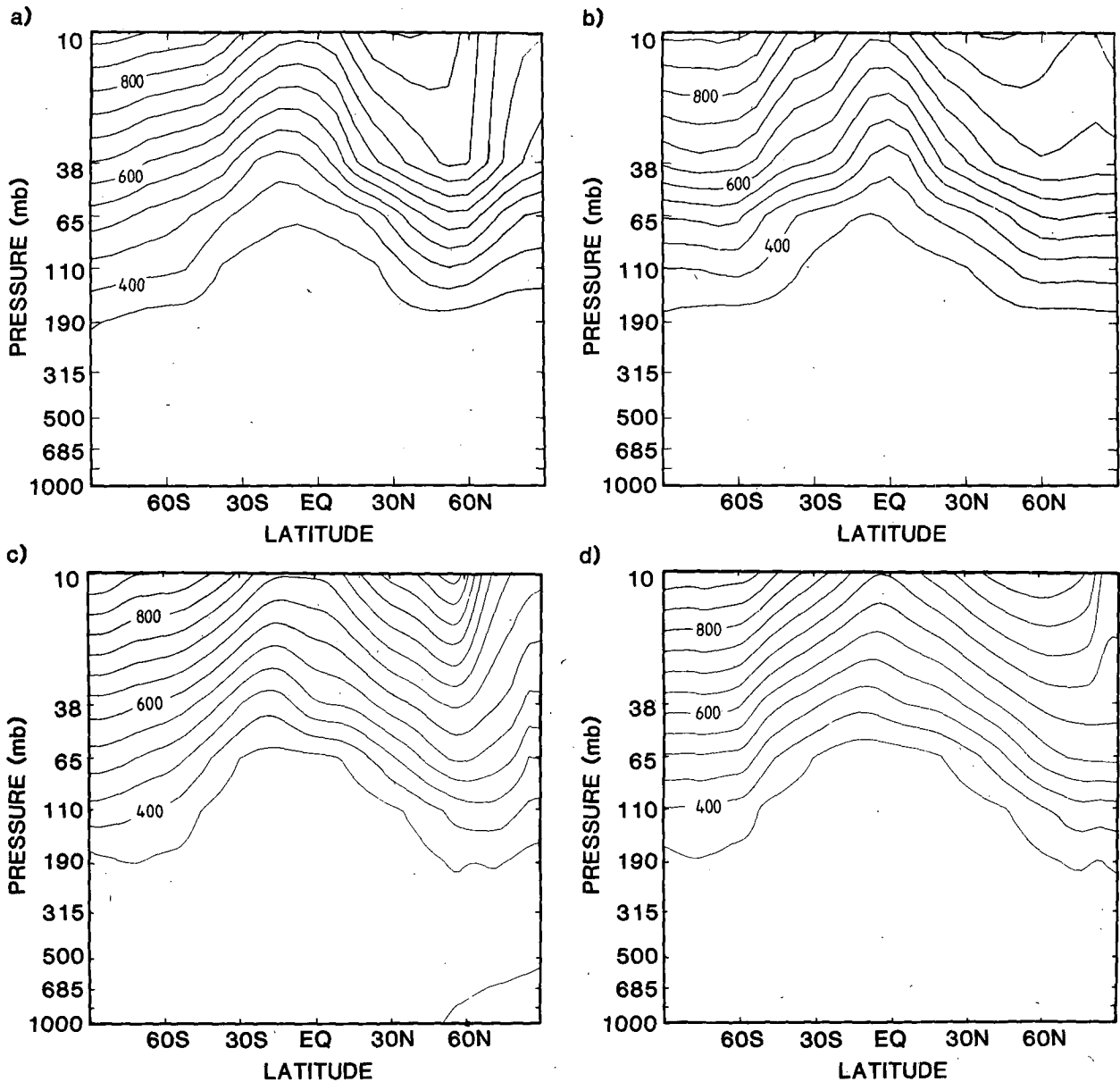a)

b)

c)

d)

FIG. 13. As in Fig. 12 but for Experiment 2.

where $z_0 = 19.68$ km, $\Delta z = 5$ km, $\phi_0 = 45°$ and $\Delta\phi = 10°$.

Rather than the parameterized wet and dry deposition scheme used by Mahlman and Moxim, a simple tropospheric sink $s = -\Lambda q$ was applied with

$$\Lambda = \begin{cases} (10\,\mathrm{d})^{-1}\dfrac{(p-300\,\mathrm{mb})}{700\,\mathrm{mb}}, & p > 300\,\mathrm{mb} \\ 0, & p \leqslant 300\,\mathrm{mb}. \end{cases}$$

The experiment was run for 37 months beginning 1 January (Yr 1). The monthly-mean $\bar{q}(\phi, z)$ at six-

monthly intervals are shown in Figs. 14 (GCM) and 15 (2D model). During the first year of the experiment [cf., Figs. 14(a)–(c) and 15(a)–(c)] the spreading of the tracer cloud poleward-downward and across the equator is reproduced extremely well by the 2D model. By the middle of the second year, however [Figs. 14(d), 15(d)] it becomes clear that the 2D model is exaggerating transport into high latitudes of the Southern Hemisphere stratosphere, a trend that continues throughout the remainder of the experiment [Figs. 14(e)–(g), 15(e)–(g)]. At about the same time, the 2D model transport down from the lower stratosphere to the tropospheric sink apparently begins to exceed that
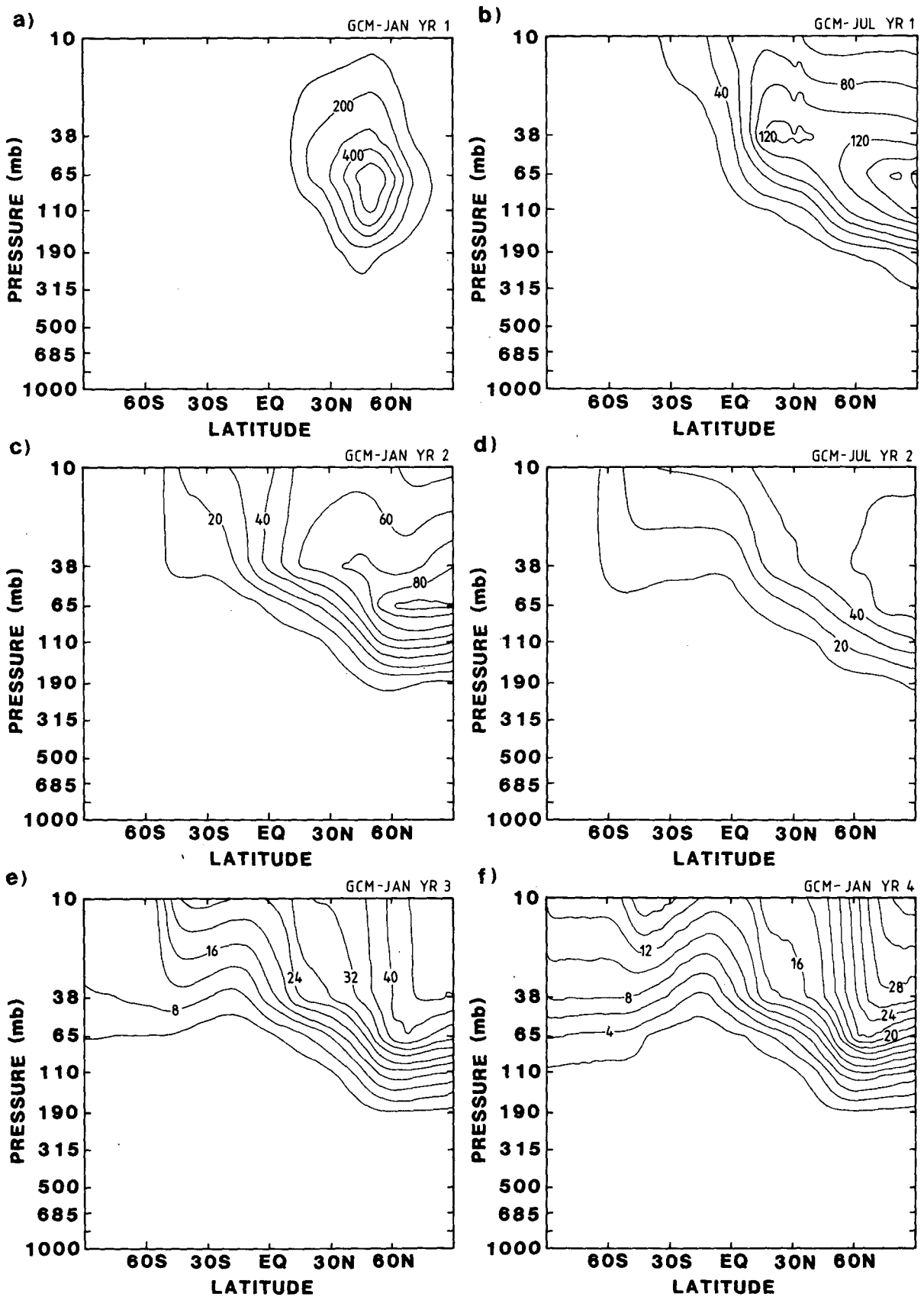
FIG. 14. Monthly mean fields of zonal-mean tracer mixing ratio for Experiment 5 from the GCM run. (a) Jan, Yr 1; (b) July, Yr 1; (c) Jan, Yr 2; (d) July, Yr 2; (e) Jan, Yr 3; (f) July, Yr 3 and (g) Jan, Yr 4.
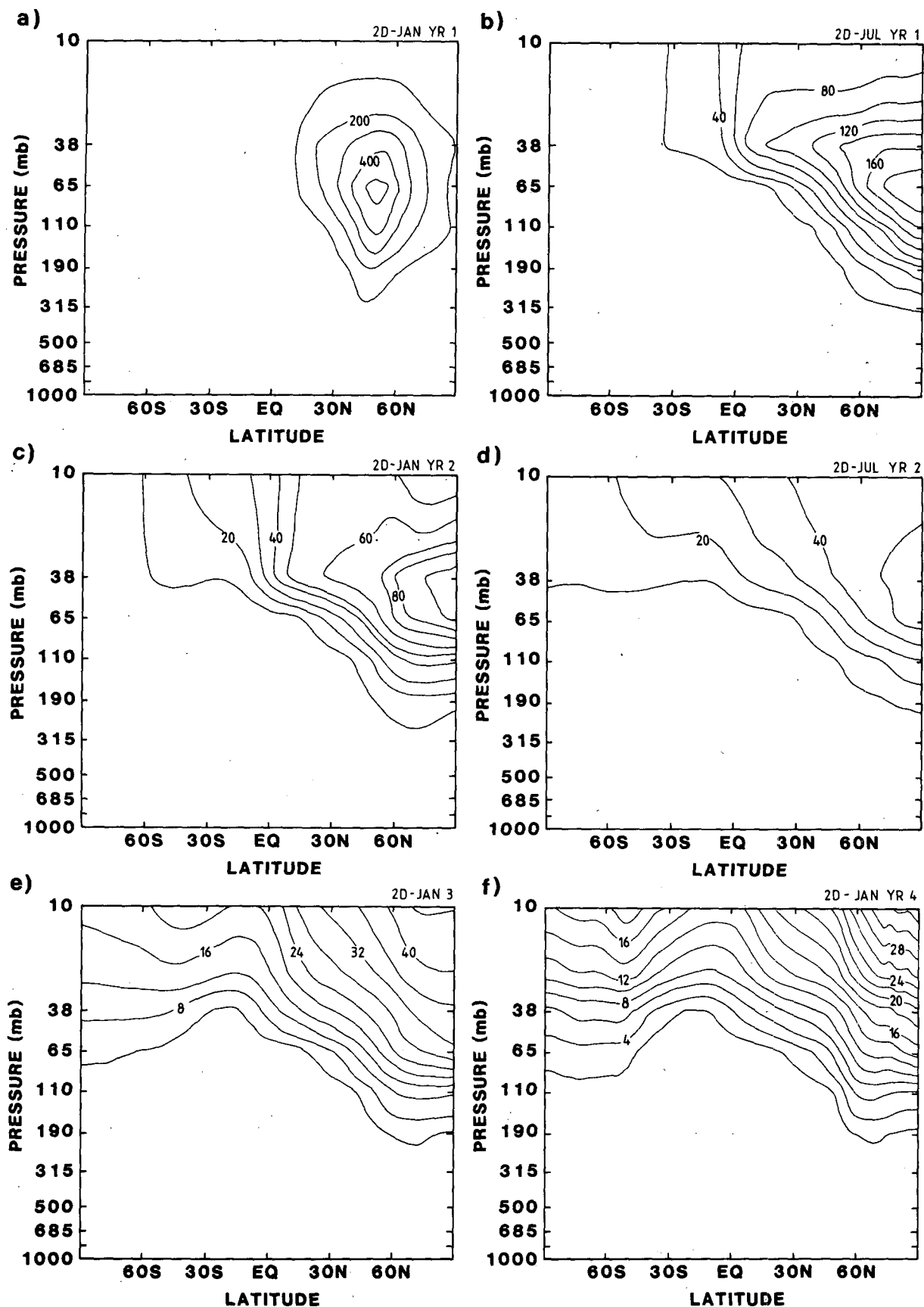
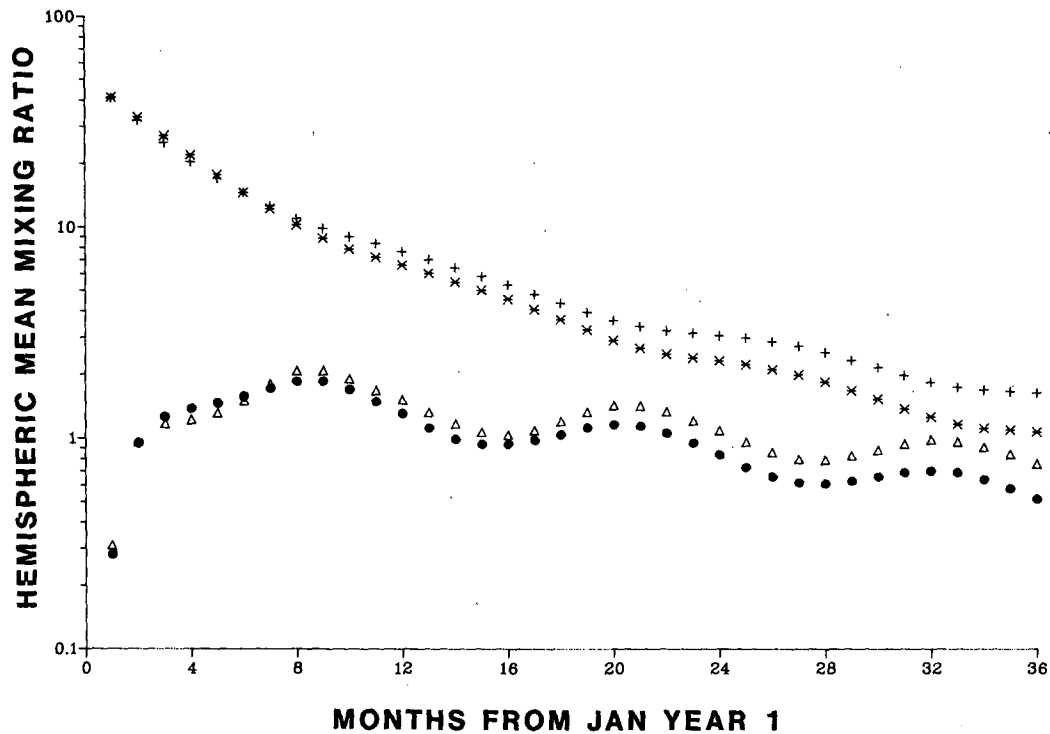FIG. 15. As in Fig. 14 but from the 2D model run.

FIG. 16. Evolution of monthly and hemispheric-mean mixing ratios from Experiment 5.
+: GCM, N.H. ✕: 2D model, N.H. △: GCM, S.H. ●: 2D model, S.H.

of the GCM experiment. This is suggested by Fig. 16; during the first year, the hemispheric mean mixing ratio in both hemispheres of the two models agree very well, but subsequently that in both hemispheres decays more rapidly in the 2D model than in the GCM. In fact, during the latter stages of the experiment, the 2D model underestimates the global tracer lifetime by about 20 percent. Despite these differences, the morphology of the model results—particularly the poleward-downward slope of isopleths in the lower stratosphere—seems to be converging in the later stages of the experiment.

This ability of the 2D model to simulate the mature structure of long-lived tracers was demonstrated further in Experiment 6, which is the "Fast-sink N_2O" experiment of Mahlman et al. (1986) to which the reader is referred for details. In this experiment a constant, zonally uniform source is specified at the surface and, in the 2D model, a sink of the form $\bar{s} = -\Lambda \bar{q}$ is specified at the two uppermost model levels; $\Lambda(\phi, z)$ was determined month-by-month by inverting this relation, given the monthly mean $\bar{s}$ and $\bar{q}$ from the final year of the GCM run. As for the GCM run, the 2D model's progress toward equilibrium was accelerated by using the updating technique of Levy et al. (1982); the magnitude of the surface source was chosen to give a mean surface mixing ratio of about 295 ppbv. The equilibrated monthly-mean fields at three-monthly intervals for the final year of the GCM and 2D model runs are

compared in Fig. 17. The value of the surface source adopted to achieve this result was 2.405×10^{13} molecules m^{-2} s^{-1}, some 22 percent higher than that required to maintain the same mean surface mixing ratio in the GCM run; this appears to be broadly consistent with the suggestion of exaggerated troposphere–stratosphere transport of the 2D model from the results of Experiment 5; however, possible errors in the representation of mean advection noted above in the region of the uppermost level could also have an impact through their influence on the flux into the sink region. As compared with the GCM results (shown in Fig. 1 of Mahlman et al., 1986), the 2D model appears to reproduce the gross features of the GCM distribution and their seasonal variation very well, in both stratosphere and troposphere. However the equatorial "tropopause" of the tracer distribution is higher (by about one vertical level) in the 2D model than in the GCM; this may be a consequence of the effective vertical smoothing of the transport coefficients noted earlier.

7. Summary and discussion

The success of the 2D model in reproducing the transport properties of the GCM lends credibility to the use of the flux-gradient parameterization to represent large-scale eddy transport of passive atmospheric tracers and therefore also to the basis of two-dimensional (zonally-averaged) tracer modeling, to within the necessary limitations of such models. The most obvious
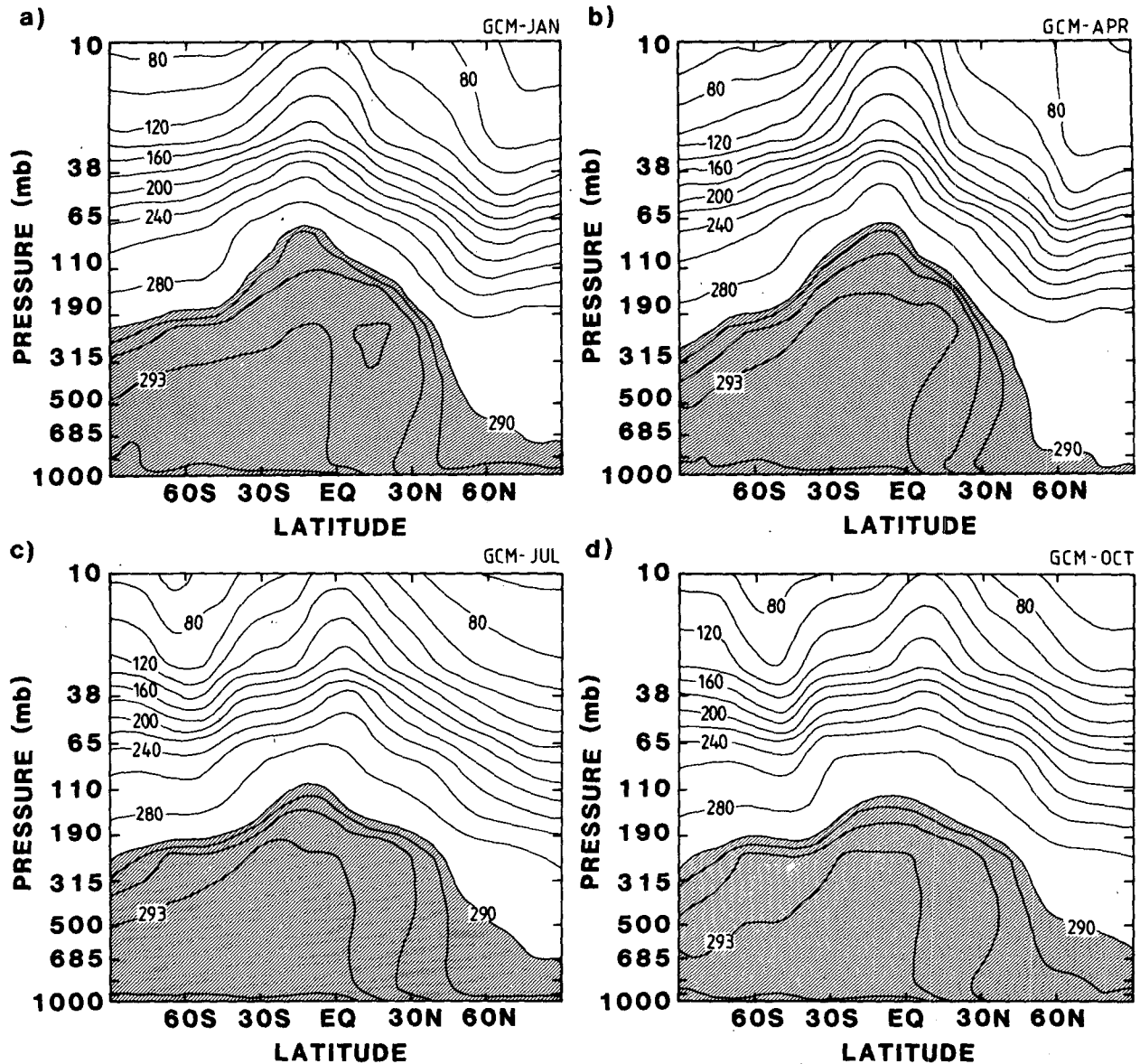
FIG. 17. Comparison of equilibrated tracer fields (ppbv) in the GCM and 2D model for Experiment 6. Monthly mean GCM results for (a) Jan (b) Apr, (c) Jul and (d) Oct; and 2D model results for (e) Jan (f) Apr (g) Jul and (h) Oct. Note different contour increments above and below 290 ppbv.

such limitation is the lack of longitudinal resolution which, among other things, precludes direct comparison with station data. A less obvious limitation is time resolution, a point touched on in section 5. It is clear, for example, that two GCM experiments, initialized with tracer distributions with identical zonal averages but different longitudinal structure, would evolve differently. A zonally-averaged model would of course see the two experiments as identical and could not therefore be expected to represent the transport correctly until the tracer distributions had become mature (i.e., with tracer isopleths approximately coincident with the large-scale streamlines). From the behavior of

experiments 3 and 4 in the early stages of evolution, it appears that the time scale for this to occur is typically 10–20 days. Since (as in most applications of zonally-averaged models) the time scales of interest in the experiments described above are much longer than this, the problem did not present any difficulties here.

Apart from their application as input to zonally-averaged models, the transport coefficients derived from the GCM experiments are of more general interest because of what they reveal of the dynamics of large-scale transport processes. The two components—advective and diffusive transport—are summarized for the model atmosphere at the solstices in Fig. 18. The simplicity
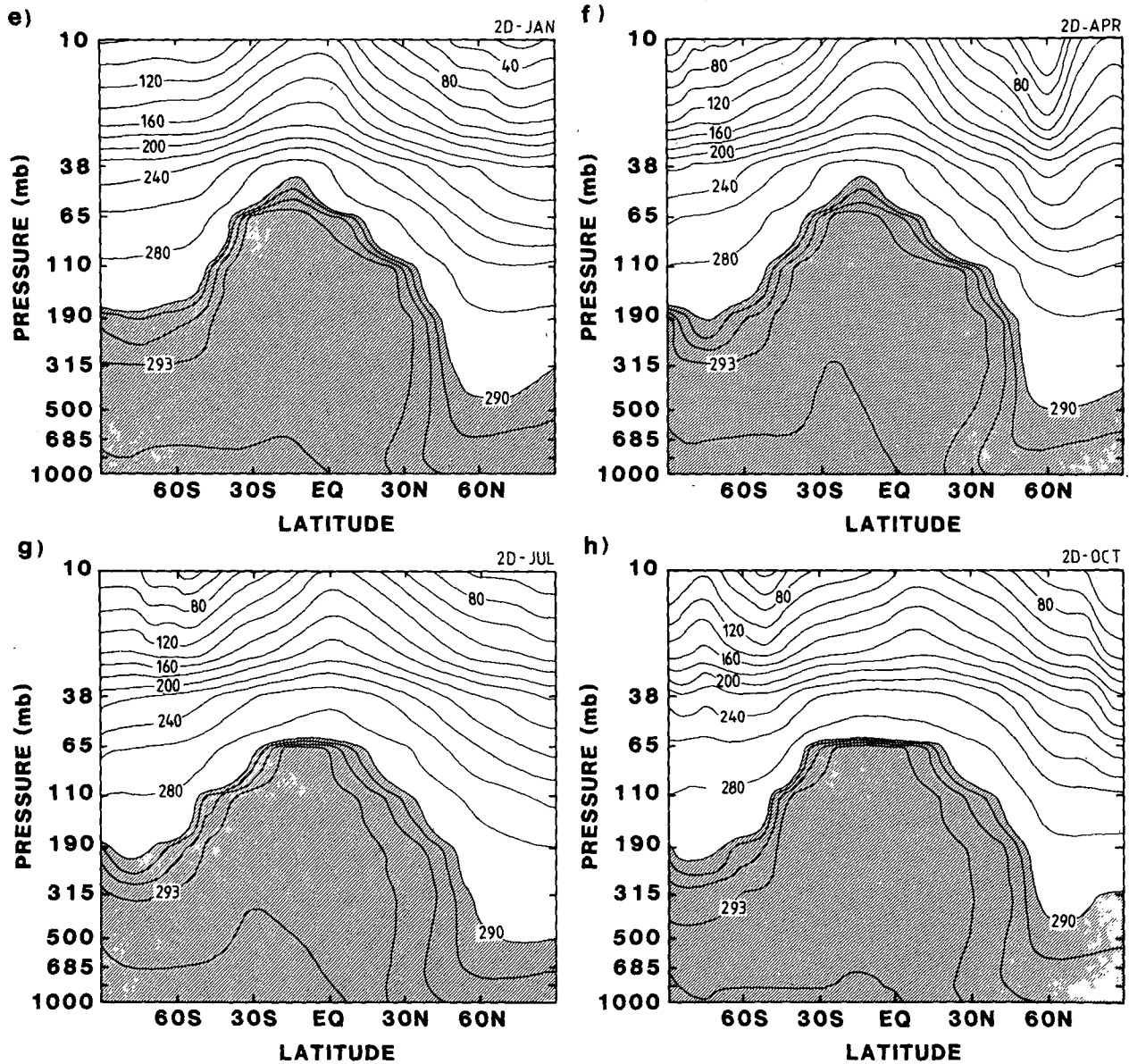
FIG. 17. (*Continued*)

of the circulation U_T has already been noted, with a two-cell Hadley-like structure in the troposphere and a single cell in the stratosphere. As such, it is structurally simpler than the Eulerian mean and even the residual mean circulations. It is also much simpler than the Lagrangian-mean circulation estimated from the transport coefficients, but qualitatively similar to that determined by Kida (1983a,b). The quasi-horizontal (quasi-isentropic) eddy mixing process are most evident in two distinct regions. The strong mixing in the mid-latitude lower troposphere is associated with transient eddies and may be an indication of the cascade processes associated with frontogenesis. The elevated band of strong mixing across the tropical upper troposphere

and into the winter subtropical stratosphere appears to be an independent confirmation of the reality of the "surf zone" identified by McIntyre and Palmer (1983, 1984)—on the basis of observed potential vorticity maps—as a manifestation of breaking quasistationary and (in the troposphere) transient planetary waves in the weak subtropical zonal winds. Strong vertical mixing is found in the tropical troposphere; vertical diffusivities are ill-determined elsewhere, though the total vertical diffusivity D_{zz} was found to be around 10 m^2 s^{-1} in much of the model troposphere.

It is of interest to compare the diffusion coefficients obtained here with some of those used hitherto in two-dimensional modelling studies. Some comparisons for
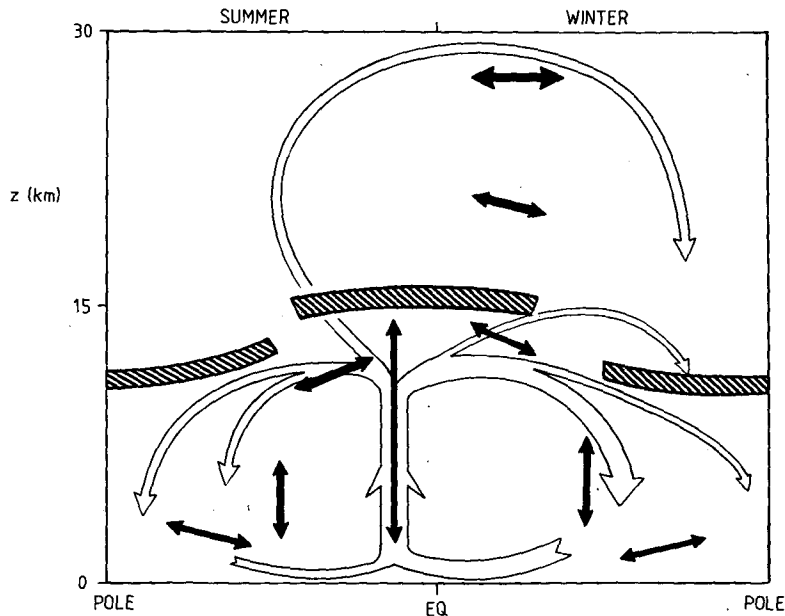
FIG. 18. Schematic representation of the transport characteristics of the GCM at the solstices. Broad arrows: major results for advective transport. Thin, double-headed arrows: major locations and directions of diffusive transport. (cf. Kida, 1983b).

D_{yy} are made in Fig. 19. (The reader is reminded that the definition used here for D_{yy} differs by a factor $\cos^2\phi$ from that used in many other studies; the values plotted here are all expressed in the present notation). In the stratosphere (Fig. 19a) the low-latitude values obtained here are surprisingly similar to those estimated by Hidalgo and Crutzen (1977) on the basis of the observed ozone distribution—surprisingly, that is, because it has been suggested in a number of recent studies that the appropriate diffusivities are much weaker than these. Kida (1983a), for example, has estimated $D_{yy} \leqslant 3 \times 10^5$ m^2 s^{-1} in the winter stratosphere, on the basis of parcel dispersion rates in a numerical model. However, it has been seen that stratospheric mixing is associated with quasi-stationary waves; Kida's model appears to be deficient in stationary wave activity—it has no orographic forcing—and, therefore, it seems likely that this value is unrepresentative. In fact Kida also found, as argued in section 2, that the effects of both advection and diffusion are formally comparable—the mean circulation is his model is also substantially weaker than that found here. Recently, however, Ko et al. (1985) have argued that the effects of diffusion in the stratosphere must be weak (through perhaps not negligible), apparently in contradiction to the present view as well as the results not only of Kida (1983a) but also of Pyle and Rogers (1980b) who found that without significant diffusion, their two-dimensional model predictions of stratospheric ozone profiles were substantially in error. This conclusion of Ko et al. was based partly on theoretical arguments (those of Tung, 1984, in which much of the quasi-stationary wave activity is

neglected and which therefore may seriously underestimate the diffusion) and partly from a comparison of model predictions of the latitudinal profile of total HNO$_3$ with observations, in which they found that a
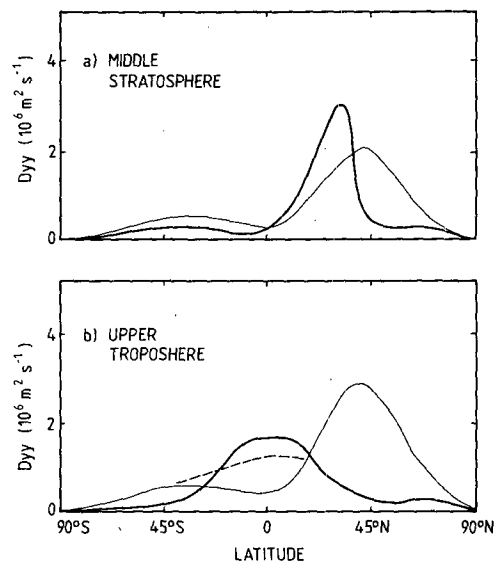

FIG. 19. Comparison of latitudinal profiles of derived horizontal diffusion coefficients for January. (a) Stratospheric values. Results of present study at about 20 mb (solid) and those of Hidalgo and Crutzen (1977) at the same level (thin solid). (b) Upper tropospheric values. Results of present study at about 240 mb (solid), those of Hidalgo and Crutzen at 200 mb (thin solid), and modifications made to the latter by Hyson et al. (1980) (dashed).

constant (in ϕ-coordinates) diffusion coefficient which in present notation becomes $D_{yy} = 1 \times 10^6 \cos^2\phi$ m^2 s^{-1} generated latitudinal gradients that were too weak. Note, however, that while the values determined in the present study are some 2–4 times larger than this in the winter subtropics, they are substantially smaller elsewhere, so that Ko et al.'s statement regarding the gross, global structure does not necessarily conflict with the present results. Indeed, the observed HNO$_3$ profiles of Gille et al. (1984) show a region of weak gradient in the winter subtropics as would be expected with strong mixing there; this reinforces the impression gained from the present study of the importance of correctly representing the *structure* of D_{yy}, and not just its typical magnitude, in zonally averaged models.

In contrast to the stratospheric comparison, the values obtained here for D_{yy} in the troposphere differ substantially from those of Hidalgo and Crutzen. These differences are most marked in the upper troposphere (Fig. 19b) where the two latitudinal profiles are strongly anticorrelated, with Hidalgo and Crutzen's values minimizing in the tropics where the present results indicate strong mixing. However, Hyson et al. (1980) found the need to increase Hidalgo and Crutzen's values in the tropics in order to obtain satisfactory model predictions of the interhemispheric gradient of CCl$_3$F. Their upper tropospheric values, also plotted in Fig. 19b, are quite similar in the tropics to those derived here.

One point that is raised by Figs. 18 and 19b relates to the often-stated view that the tropics act as a throttle to interhemispheric exchange. The properties of tropospheric transport revealed in the GCM contradict this view. The route for transport from the midlatitudes of one hemisphere into the other (see Fig. 18) is

(i) into the intertropical convergence by lower tropospheric advection

(ii) upward advection and diffusion, and then

(iii) outward into the upper troposphere of both hemispheres, again via both advective and diffusive processes. As is clear from the results of Experiment 1, this process is very rapid; indeed it would appear that the time scale for exchange between high latitudes of the two hemispheres is limited by the time scale for transport into the tropics (or, for a midlatitude source, by the time scale for the Hadley cell, in its seasonal migration, to move close to the source region) rather than that for transport across the tropics. (Of course, a particulate or soluble tracer would be strongly depleted by wet removal processes in the tropics, but that is another question.)

The transport coefficients derived in this study are, by design, representative of the dispersion of conserved tracers in the model. As discussed in section 2, however, additional diffusive effects arise for nonconserved constituents. To what extent these so-called "chemical eddy" terms are important depends on the relative magnitudes of the two effects. Rogers and Pyle (1984) have calculated horizontal diffusivities arising from the chemical relaxation effect (only) for ozone; their values are typically less than 1×10^6 m^2 s^{-1} in low and middle latitudes of the winter stratosphere and so it appears that the dispersion effect represented by the present results will dominate, at least in the subtropics. Further, as will be discussed below, it seem likely that the GCM underestimates the transport in the high latitude winter stratosphere, so that even there dispersion may dominate. Therefore the present results may be applicable to all stratospheric tracers (at least below 10 mb) whose lifetimes are comparable with or longer than that of ozone.

Of course, the best that can be expected of the derived zonally-averaged model (and we have seen that it approaches this expectation) is that it will reproduce the zonally-averaged behavior of the parent GCM, including its shortcomings. The impact of some of these shortcomings is difficult to assess. The apparent impact of the upper lid at 10 mb on vertical transport in the upper levels of the model has been discussed by Mahlman et al. (1986) on the basis of the model's performance in simulating the distribution of N$_2$O. Another potentially serious shortcoming of this model (and most others) is the absence of high-latitude stratospheric warming events. It seems likely that the impact of this on the present results is that the derived transport coefficients are too weak in high latitudes, especially in late winter. However, there are some indications that the large values derived for D_{yy} in the winter subtropics are reasonable. During early winter, the gradient of quasi-geostrophic potential vorticity is eroded in the winter subtropics; this process has become known as "preconditioning" because it is believed to be a necessary precursor to subsequent high-latitude warming events (see McIntyre, 1982). As was discussed in section 3, only the diffusive component of transport influences the quasigeostrophic potential vorticity budget. Mixing over the length scale of 3×10^6 m in a time scale of about 50 days implies a diffusion coefficient of $L^2/T \approx 2 \times 10^6$ m^2 s^{-1}, very much in line with the values determined here. If the magnitude of D_{yy} were as small as some of the suggested values noted above, preconditioning could not occur in the time available (a winter season).

While no assumptions were made a priori in this derivation, the results obtained for the model stratosphere largely support the assumptions of Mahlman et al. (1981) and Tung (1982, 1984); viz, the diffusion is approximately along the isentropic surfaces and the transport circulation is reasonably well approximated by the residual circulation. Therefore, notwithstanding the near impossibility of deriving the complete transport coefficients from observed circulation data, one may be able to construct a soundly based model via the flux-gradient approach used here. Specifically, given calculations of D_{yy} from, say, the flux of quasigeo-

strophic potential vorticity, D_{yz} could be estimated from the isentropic slopes. A calculation of the residual circulation and an assumption that vertical diffusion is negligible would complete the set of required coefficients, assuming that D_{zz} is negligible in the stratosphere. This procedure has been adopted by Newman et al. (1986).

REFERENCES

Andrews, D. G., and M. E. McIntyre, 1976: Planetary waves in horizontal and vertical shear: the generalized Eliassen-Palm relation and the mean zonal acceleration. *J. Atmos. Sci.*, **33**, 2031–2048.

Andrews, D. G., and M. E. McIntyre, 1978: An exact theory of nonlinear waves on a Lagrangian mean flow. *J. Fluid. Mech.*, **89**, 609–646.

Clark, J. H. E., and T. G. Rogers, 1978: The transport of conservative trace gases by planetary waves. *J. Atmos. Sci.*, **35**, 2232–2235.

Clough, S. A., N. S. Grahame and A. O'Neill, 1985: Potential vorticity in the stratosphere derived using data from satellites. *Quart. J. Roy. Meteor. Soc.*, **111**, 335–358.

Danielsen, E. F., 1981: An objective method for determining the generalized transport tensor for two-dimensional Eulerian models. *J. Atmos. Sci.*, **38**, 1319–1339.

Dunkerton, T., 1980: A Lagrangian mean theory of wave–mean flow interaction with applications to nonacceleration and its breakdown. *Rev. Geophys. Space Phys.*, **18**, 387–400.

Edmon, H. J., Jr., B. J. Hoskins and M. E. McIntyre, 1980: Eliassen-Palm cross-sections for the troposphere. *J. Atmos. Sci.*, **37**, 2600–2616.

Fels, S. B., J. D. Mahlman, M. D. Schwarzkopf and R. W. Sinclair, 1980: Stratospheric sensitivity to perturbations in ozone and carbon dioxide: radiative and dynamical response. *J. Atmos. Sci.*, **37**, 2265–2297.

Garcia, R. R., and S. Solomon, 1983: A numerical model of the zonally averaged dynamical and chemical structure of the middle atmosphere. *J. Geophys. Res.*, **88**, 1379–1400.

Gille, J. C., J. M. Russel III, P. L. Bailey, E. E. Remsberg, L. L. Gordley, W. F. J. Evans, H. Fischer, B. W. Gandrud, A. Girard, J. E. Harries and S. A. Beck, 1984: Accuracy and precision of the nitric acid concentrations determined by the Limb Infrared Monitor of the Stratosphere experiment on NIMBUS 7. *J. Geophys. Res.*, **89**, 5179–5190.

Guthrie, P. D., C. H. Jackman, J. R. Herman and C. J. McQuillan, 1984: A diabatic circulation experiment in a two-dimensional photochemical model. *J. Geophys. Res.*, **89**, 9589–9602.

Hartmann, D. L., and R. R. Garcia, 1979: A mechanistic model of ozone transport by planetary waves in the stratosphere. *J. Atmos. Sci.*, **36**, 350–364.

Held, I. M., and A. Y. Hou, 1980: Nonlinear axially symmetric circulations in a nearly inviscid atmosphere. *J. Atmos. Sci.*, **37**, 515–535.

Hidalgo, H., and P. J. Crutzen, 1977: The tropospheric and stratospheric composition perturbed by NO_x emissions of high-altitude aircraft. *J. Geophys. Res.*, **82**, 5833–5866.

Holloway, G., and S. S. Kristmannsson, 1984: Stirring and transport of tracer fields by geostrophic turbulence. *J. Fluid. Mech.*, **141**, 27–50.

Holton, J. R., 1981: An advective model for two-dimensional transport of stratospheric trace species. *J. Geophys. Res.*, **86**, 11 989–11 994.

Hsu, C.-P., 1980: Air parcel motions during a numerically simulated stratospheric warming. *J. Atmos. Sci.*, **37**, 2768–2792.

Hyson, P., P. J. Fraser and G. I. Pearman, 1980: A two-dimensional transport simulation model for trace atmospheric constituents. *J. Geophys. Res.*, **85**, 4443–4445.

Kida, H., 1983a: General circulation of air parcels and transport characteristics derived from a hemispheric GCM. Part 1. A determination of advective mass flow in the lower stratosphere. *J. Meteor. Soc. Japan*, **61**, 171–187.

——, 1983b: General circulation of air parcels and transport characteristics derived from a hemispheric GCM. Part 2. Very long-term motions of air parcels in the troposphere and stratosphere. *J. Meteor. Soc. Japan*, **61**, 510–523.

Ko, M. K. W., K. K. Tung, D. K. Weisenstein and N. D. Sze, 1985: A zonal mean model of stratospheric tracer transport in isentropic coordinates: numerical simulations for nitrous oxide and nitric acid. *J. Geophys. Res.*, **90**, 2313–2329.

Kohno, J., 1984: Stratospheric ozone transport due to transient large-amplitude planetary waves. *J. Meteor. Soc. Japan*, **62**, 413–439.

Kurzeja, R. J., 1981: The transport of trace chemicals by planetary waves in the stratosphere. Part 1. Steady waves. *J. Atmos. Sci.*, **38**, 2779–2788.

Leovy, C. B., C.-R. Sun, M. H. Hitchman, E. E. Remsberg, J. M. Russell III, L. L. Gordley, J. C. Gille and L. V. Lyjak, 1985: Transport of ozone in the middle stratosphere: evidence for planetary wave breaking. *J. Atmos. Sci.*, **42**, 230–244.

Lettau, H., 1951: Diffusion in the upper atmosphere. *Compendium of Meteorology*, T. F. Malone, Ed., Amer. Meteor. Soc., 320–333.

Levy, H. II, J. D. Mahlman and W. J. Moxim, 1982: Tropospheric N_2O variability. *J. Geophys. Res.*, **87**, 3061–3080.

——, J. D. Mahlman, W. D. Moxim and S. C. Liu, 1985: Tropospheric ozone: the role of transport. *J. Geophys. Res.*, **90**, 3753–3772.

Mahlman, J. D., 1985: Mechanistic interpretation of stratospheric tracer transport. *Advances in Geophysics*, Vol. 28, *A. Climate Dynamics*, B. Saltzman, Ed., Academic Press, 301–320.

——, and W. J. Moxim, 1978: Tracer simulation using a global general circulation model: results from a midlatitude instantaneous source experiment. *J. Atmos. Sci.*, **35**, 1340–1374.

——, H. Levy II and W. J. Moxim, 1980: Three-dimensional tracer structure and behaviour as simulated in two ozone precursor experiments. *J. Atmos. Sci.*, **37**, 655–685.

——, —— and ——, 1986: Three-dimensional simulations of stratospheric N_2O: predictions for other trace constituents. *J. Geophys. Res.*, **91**, 2687–2707.

——, D. G. Andrews, D. L. Hartmann, T. Matsuno and R. G. Murgatroyd, 1981: Transport of trace constituents in the stratosphere. Report of Study Group 2. *Handbook for MAP*, **3**, 14–43. [Also appears in "Dynamics of the Middle Atmosphere," J. R. Holton and T. Matsuno, eds., pp. 387–415. Terrapub, Tokyo (1984)].

Manabe, S., and J. D. Mahlman, 1976: Simulation of seasonal and interhemispheric variations in the stratospheric circulation. *J. Atmos. Sci.*, **33**, 2185–2217.

Matsuno, T., 1980: Lagrangian motion of air parcels in the stratosphere in the presence of planetary waves. *Pure Appl. Geophys.*, **118**, 189–216.

McIntyre, M. E., 1980: Towards a Lagrangian-mean description of stratospheric circulations and chemical transports. *Phil. Trans. Roy. Soc. London*, **A296**, 129–148.

——, 1982: How well do we understand the dynamics of stratospheric warmings? *J. Meteor. Soc. Japan*, **60**, 37–65.

——, and T. N. Palmer, 1983: Breaking planetary waves in the stratosphere. *Nature*, **305**, 593–594.

——, and ——, 1984: The "surf zone" in the stratosphere. *J. Atmos. Terr. Phys.*, **46**, 825–849.

Newman, P. A., M. R. Schoeberl and R. A. Plumb, 1986: Horizontal mixing coefficients calculated from National Meteorological Center data. *J. Geophys. Res.*, **91**, 7919–7924.

Plumb, R. A., 1979: Eddy fluxes of conserved quantities by small-amplitude waves. *J. Atmos. Sci.*, **36**, 1699–1704.

——, 1982: The circulation of the middle atmosphere. *Aust. Meteor. Mag.*, **30**, 107–121.

Pyle, J. A., and C. F. Rogers, 1980a: Stratospheric transport by stationary planetary waves: the importance of chemical processes. *Quart. J. Roy. Meteor. Soc.*, **106**, 421–446.

——, and ——, 1980b: A modified diabatic circulation model for stratospheric diffusion by large-scale mixing. *Mon. Wea. Rev.*, **93**, 313–321.

Reed, R. J., and K. E. German, 1965: A contribution to the problem of stratospheric diffusion by large-scale mixing. *Mon. Wea. Rev.*, **93**, 313–321.

Rogers, C. F., and J. A. Pyle, 1984: Stratospheric tracer transport: a modified diabatic circulation model. *Quart. J. Roy. Meteor. Soc.*, **110**, 219–237.

Simmons, A. J., and B. J. Hoskins, 1978: The life cycles of some nonlinear baroclinic waves. *J. Atmos. Sci.*, **37**, 1679–1684.

Solomon, S., and R. R. Garcia, 1984: On the distribution of long-lived tracers and chlorine species in the middle atmosphere. *J. Geophys. Res.*, **89**, 11 633–11 644.

Tuck, A. F., 1979: A comparison of one, two and three-dimensional model representations of stratospheric gases. *Phil. Trans. Roy. Soc. London*, **A290**, 477–498.

Tung, K. K., 1982: On the two-dimensional transport of stratospheric trace gases in isentropic coordinates. *J. Atmos. Sci.*, **39**, 2330–2355.

——, 1984: Modelling of tracer transport in the middle atmosphere. *Dynamics of the Middle Atmosphere*, J. R. Holton and T. Matsuno, Eds., Terrapub, pp. 417–444.

Wallace, J. M., 1978: Trajectory slopes, countergradient heat fluxes and mixing by lower stratospheric waves. *J. Atmos. Sci.*, **35**, 554–558.